DOE/CS/10510-T9

THE STUDY OF CORROSION IN MULTIMETALLIC SYSTEMS

Task 2 of Solar Collector Studies for Solar Heating and Cooling Applications

Final Technical Progress Report

By
Ronald B. Diegle

April 11, 1980

Work Performed Under Contract No. AC04-79CS10510

Battelle
Columbus Laboratories
Columbus, Ohio

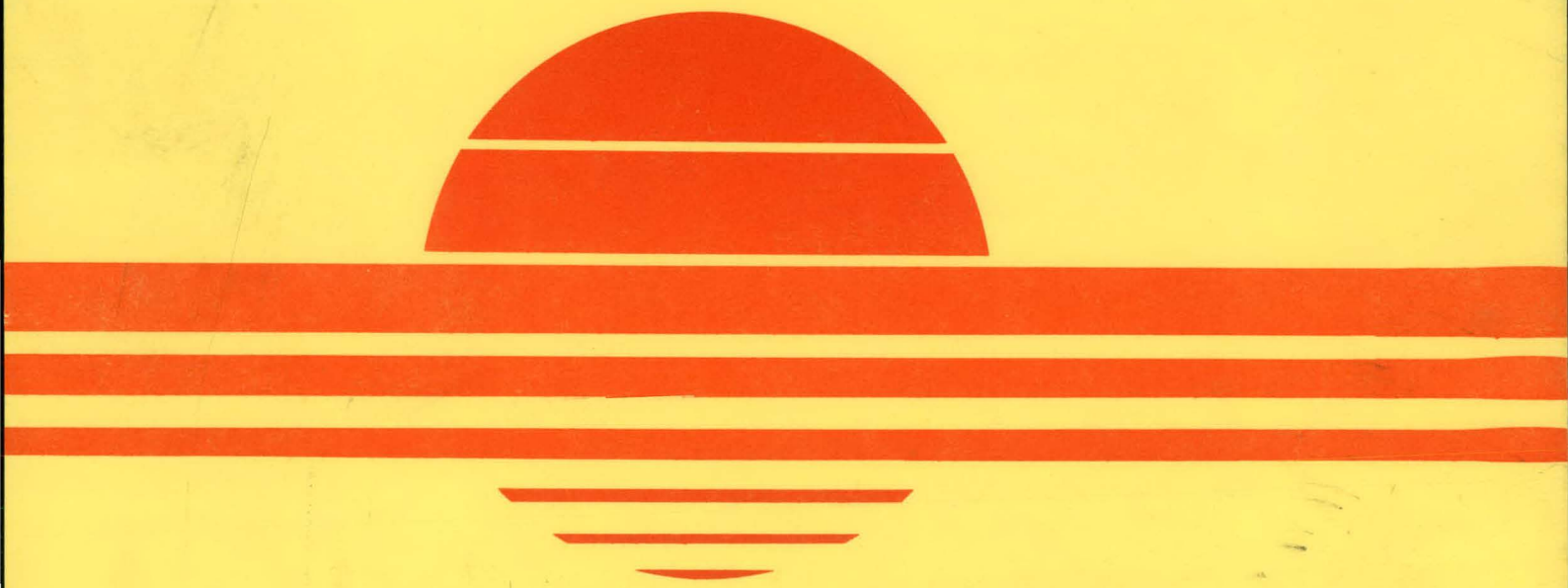

U.S. Department of Energy

Solar Energy

DISCLAIMER

DISCLAIMER

Available from the National Technical Information Service, U. S. Department of Commerce, Springfield. Virginia 22161.

Price: Paper Copy $7.00
Microfiche $3.50

DOE/CS/10510-T9
Distribution Categories UC-59 and UC-59c

FINAL
TECHNICAL PROGRESS REPORT

on

THE STUDY OF CORROSION IN MULTIMETALLIC SYSTEMS

TASK 2 OF SOLAR COLLECTOR STUDIES FOR SOLAR HEATING AND COOLING APPLICATIONS

to

U.S. DEPARTMENT OF ENERGY

April 11, 1980

by

Ronald B. Diegle

Contract No. DE-AC04-79CS10510

BATTELLE
Columbus Laboratories
505 King Avenue
Columbus, Ohio 43201

TABLE OF CONTENTS

TABLE OF CONTENTS
(Continued)

Page

APPENDIX

LIST OF TABLES

LIST OF FIGURES

ABSTRACT

Corrosion measurements were made on candidate alloys of construction for non-concentrating solar collectors under simulated conditions of collector operation. Materials evaluated were aluminum alloys 1100, 3003, and 6061, copper alloy 122, Type 444 stainless steel, and 1018 plain carbon steel. The solutions used were equivolume mixtures of ethylene glycol and water, and propylene glycol and water. They were used without corrosion inhibitors but with addition of chloride, sulfate, and bicarbonate ions. The influences of dissolved oxygen, solution flow velocity, and heat transfer were evaluated. Corrosion morphologies investigated were general attack, pitting, crevice corrosion, and galvanic corrosion. Experimental results indicated that aluminum alloys can experience severe pitting and crevice corrosion at chloride concentrations approaching 50 ppm. The corrosion rate of copper exceeded about 100 μm/yr in ethylene glycol solutions and about 80 μm/yr in propylene glycol solutions. Crevice corrosion was not observed for copper, but severe galvanic corrosion occurred when it was coupled to T444 stainless steel. T444 steel corroded at rates of less than 1 μm/yr under all exposure conditions. During circulation at 100 C in the presence of air, ethylene glycol solutions acidified because of degradation of the glycol. The initial pH of propylene glycol solutions was already low, about 4.5. The inherent corrosivity of propylene glycol was somewhat less than that of ethylene glycol, although this difference was usually less than a factor of two in measured corrosion rates. It was concluded that the corrosion rates of aluminum alloys and copper were prohibitively high in uninhibited glycol solutions, and that corrosion inhibitors are definitely necessary in operating systems. It may not be necessary to use corrosion inhibitors in T444 stainless steel collectors.

FINAL
TECHNICAL PROGRESS REPORT

on

THE STUDY OF CORROSION IN MULTIMETALLIC SYSTEMS

to

U.S. DEPARTMENT OF ENERGY

from

BATTELLE
Columbus Laboratories

by

Ronald B. Diegle

April 11, 1980

INTRODUCTION

To insure the integrity of solar collector systems for a design lifetime of ten years or longer, it is necessary to minimize and control the detrimental effects of corrosion. The purpose of this DOE-sponsored research program is to characterize the corrosion behavior of candidate alloys of construction for solar collectors under simulated service conditions. The program included three separate tasks, as follows:

(1) Review of the state of the art of collector corrosion
(2) Study of aqueous corrosion in multimetallic systems under simulated solar collector operating conditions
(3) Determination of the interactions between constituents in various kinds of waters and chemical antifreeze additives.

This report describes results from the second task; results from the other two appear in separate technical progress reports[1,2].

Scope of Task 2

This research involved characterizing corrosion of different metals and alloys in simulated tap waters of varying ionic strength. The metals and alloys were selected based on results of the Task 1 literature survey[1]; they consisted of copper, plain carbon steel, stainless steel (Type 444), and aluminum alloys (1100, 3003, 6061). The waters contained antifreeze additions that were determined most likely to be used in aqueous collector coolants, again based on results of the Task 1 literature review. Exposure conditions simulated the more severe range of those likely to be encountered in residential heating and cooling applications in a non-concentrating solar collector system.

Primarily because of time constraints in this research program, it was necessary to limit the scope of experimental work within well-defined limits. Specifically, in order to obtain measurable corrosion within reasonable exposure times of two to three weeks, rather severe operating conditions were investigated. Thus, no corrosion inhibitors were evaluated, this being reserved for subsequent investigations. Ranges in pertinent variables included temperatures to 100 C, Reynolds numbers to 7000, aeration and deaeration, and a range of water chemistries with ethylene and propylene glycol. Many experiments were performed in a recirculating system that simulated certain performance aspects of non-concentrating collectors; stagnation, however, was investigated only in Task 3 research. Related research involved evaluating susceptibility to crevice corrosion and galvanic coupling effects.

Evaluation of corrosion inhibitors was outside the scope of this program because the philosophy of this research was to study the most severe exposure conditions that reasonably could be expected to be encoun- during operation of residential non-concentrating solar collectors.

One of these conditions was depletion of corrosion inhibitors and buffer capacity from the coolant, which can occur in inadequately maintained systems containing (initially) inhibited coolant. Because of the absence of corrosion inhibitors and the use of other non-ideal conditions, such as air saturation and presence of chloride ions, the results of this research indicate materials performance under relatively harsh operating conditions.

PROJECT OBJECTIVES

The specific objectives of Task 2 research were as follows:

(1) Determine corrosion behavior of candidate alloys of construction of low temperature solar collectors in candidate collector coolants.

(2) Determine long term corrosion effects in these coolants, including identification of metals that are most effective under various conditions of exposure.

(3) Determine the effects of galvanic coupling by various metal combinations.

(4) Determine the susceptibility of these metals to crevice corrosion.

EXPERIMENTAL PROCEDURES

Materials

A survey of published literature in the Task I Report[1] and communications with representatives of various metals producers resulted

in identification of six metals or alloys for experimental evaluation. These alloys were identified as either already in use in commercial non-concentrating collectors, or likely candidates for future use. They are: copper alloy CDA 122; aluminum alloys 1100, 3003, and 6061; Type 444 stainless steel; and plain carbon steel. Their nominal compositions are given in Table 1. Specimens used in the recirculating system were in the form of tubing, each 17.8 cm (7 in.) long, 0.953 cm (0.375 in.) outside diameter, and 0.755 cm (0.305 in.) inside diameter. Galvanic coupling and crevice corrosion experiments were performed on specimens cut from sheet stock, which was not necessarily from the same heats as the tubular specimens.

All specimens were chemically etched to establish standard, reproducible, and uniform surface conditions. These treatments were as follows: (1) for aluminum alloys, a two-minute immersion in 10 percent NaOH at 22 C; (2) for copper, a one-minute immersion in 10 percent HNO_3 at 22 C; (3) for T444 stainless steel, a ten-minute immersion in 10 percent HF plus 20 percent HNO_3 at 60 C; and (4) for 1018 steel, a fifteen-second immersion in 10 percent HNO_3 at 22 C. The specimens were rinsed and oven dried at 100 C, and the tubular samples then were weighed to the nearest 0.0001 gram prior to exposure.

The literature review[1] indicated that the most promising aqueous coolants were ethylene glycol/water and propylene glycol/water mixtures. The glycols were of reagent grade purity. The water was either distilled, or else it was a full strength or diluted solution originally containing 148 mg/l of Na_2SO_4, 165 mg/l of NaCl, and 138 mg/l of $NaHCO_3$ in distilled water, referred to as "ASTM water". This solution, described in ASTM Specification D2570, contained 100 ppm each of Cl, SO_4, and HCO_3 ions prior to dilution with glycol. The glycol/water mixtures were made with equal volumes of glycol and water.

Corrosion Under Dynamic Flow

Data obtained under dynamic flow conditions were generated in the recirculating system shown schematically in Figure 1. This system

TABLE 1. NOMINAL COMPOSITIONS OF METALS AND ALLOYS USED IN THIS RESEARCH PROGRAM

Metal	Concentration, Weight Percent															
	Si	Fe	Cu	Mn	Mg	Cr	Zn	Ti	Nb	Al	Mo	C	N	P	S	Wt
Al 1100	1.0 Si + Fe (Maximum)		0.05-0.20	0.05			0.10			≥ 99						
Al 3003	0.6	≤ 0.07	0.05-0.20	1.0 -1.5			0.10			Bal.						
Al 6061	0.40-0.80	≤ 0.07	0.15-0.40	0.15	0.8-1.2	0.04-0.35	0.25	0.15		Bal.						
Cu 122										≥ 99.8				0.02		
T444 Stainless Steel	0.14		0.08	0.24		18.85		0.12	0.89		2.00	0.019	0.020	0.025	0.005	0.49
1018 Steel				0.60-0.90								0.15-0.20		≤ 0.04	≤ 0.05	

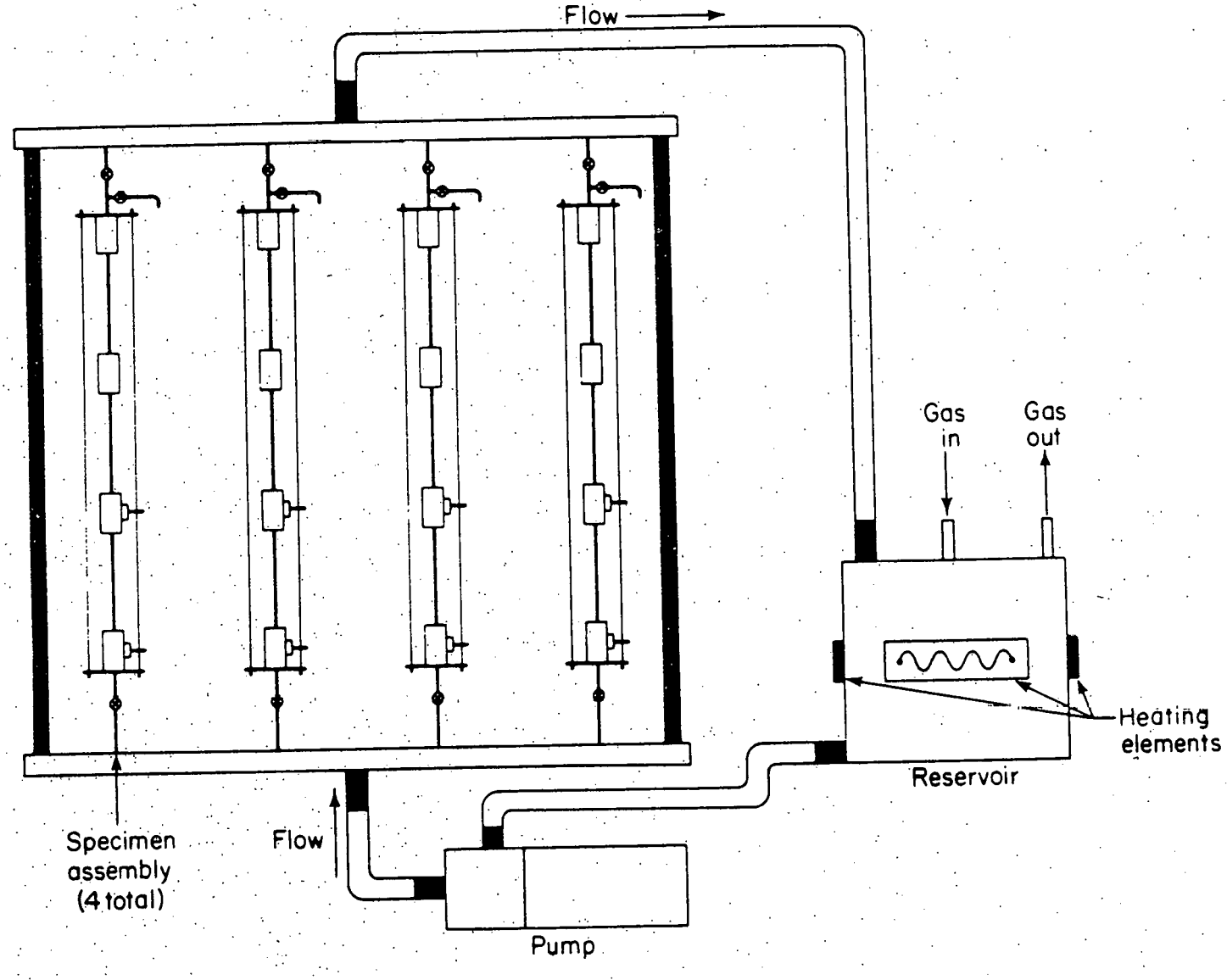

FIGURE 1. RECIRCULATING SYSTEM USED TO OBTAIN CORROSION DATA UNDER DYNAMIC FLOW CONDITIONS

duplicated many aspects of a typical flat plate solar collector. It consisted of four specimen assemblies through which coolant circulated, a 20-liter reservoir, and a pump. During operation, the solution was pumped from the heated reservoir into the inlet header tube, through the four parallel specimen assemblies, into the exit header tube, and back to the reservoir for reheating and recycling. Figure 2 shows a more detailed view of the arrangement of the four specimen assemblies.

The flow rate of 61 cm/sec (2 ft/sec) corresponds to Reynolds numbers, N_{Re}, of 1050 and 6880 for an EG/water mixture (50:50 by volume) at 22 and 100 C, respectively, and N_{Re} of 760 and 5910 for a similar PG/water mixture at these same respective temperatures. Thus, the majority of exposure time during each experiement involved turbulent flow for both types of glycol solutions. Typically, the solutions were equilibrated with air during the exposure except for the last ten to twenty percent of the total time, during which nitrogen was used above the solution to indicate the effects of deaeration on corrosion rate.

The pump head and all transfer tubing were made of polytetrafluoroethylene (Teflon, PTFE). The header tubes were made of Hastelloy C-276 (HC-276), and the valves were constructed from stainless steel. The titanium reservoir was equipped with external electrical resistance heating elements, internal thermocouple well, and ports for aeration, or deaeration by nitrogen. Gas, either air or tank nitrogen, was passed through the reservoir continuously during each experiment. Solution flow rate was adjusted by means of the upper row of valves in the specimen assembly rack. Samples of solution were withdrawn periodically through a drain valve for pH determination. Inlet and outlet solution temperatures were monitored continuously by means of external thermocouples; the outlet temperature was controlled at 99 to 100 C. All parts of the system, including the specimens, were thermally insulated to minimize heat loss from the solution. In two experiments the effect of heat transfer through the specimens to the solution was investigated.

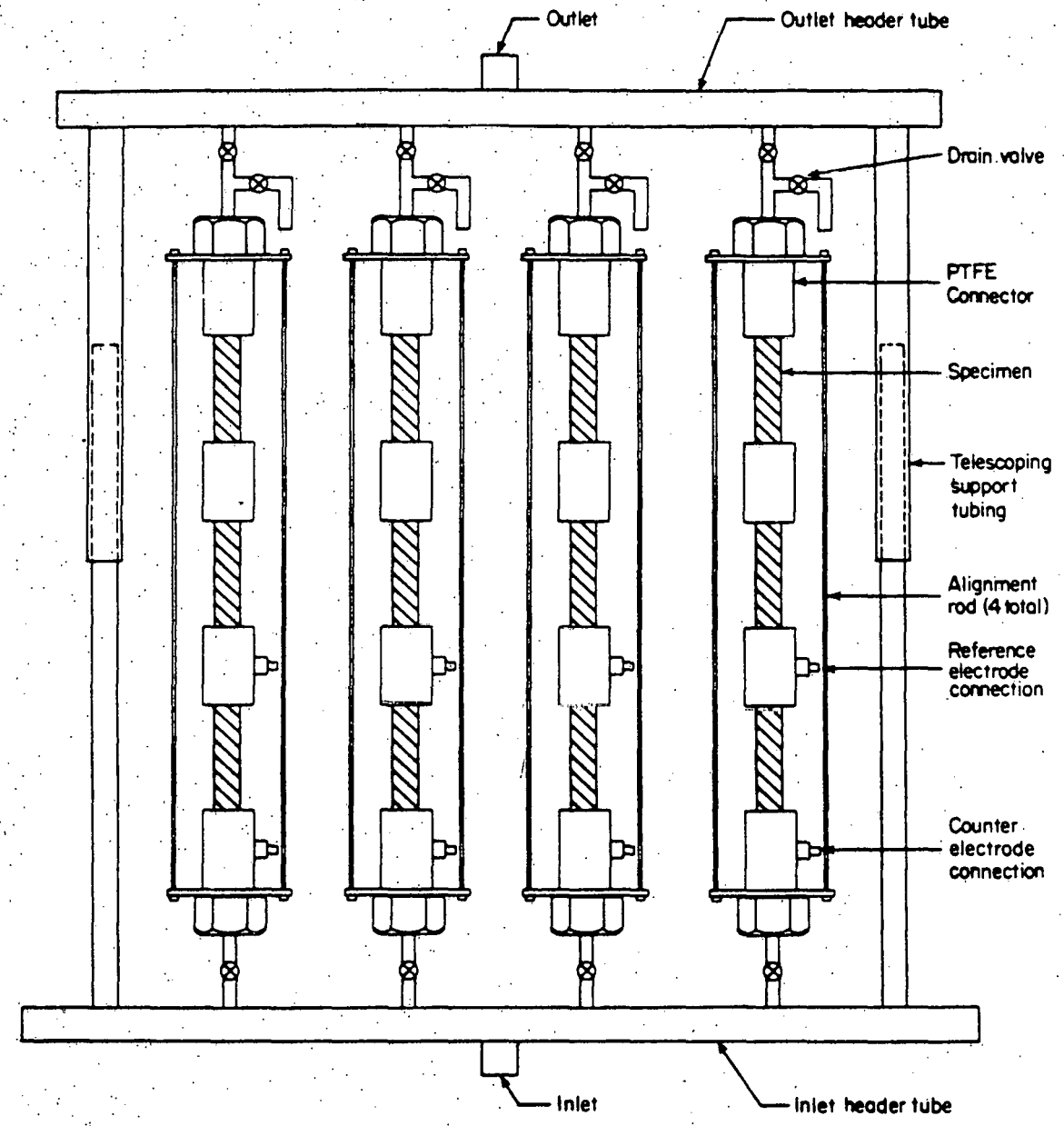

FIGURE 2. SPECIMEN ASSEMBLY RACK AND SPECIMEN ASSEMBLIES

A cross sectional view of a specimen assembly is shown in Figure 3. The bottom specimen in each assembly contained a 0.159 cm (0.0625 in.) Hastelloy C-276 rod that served as a counterelectrode for polarization resistance (PR) measurements. A string bridge penetrated the PTFE connector situated above the bottom tube specimen and connected with a saturated calomel electrode (SCE) at ambient temperature.

Crevice Corrosion

Crevice corrosion susceptibility was evaluated with the assemblies depicted in Figure 4. The ratio of total metal-metal crevice area to the area of freely exposed metal surface was 1:10. The PTFE spacers served not only as electrical insulators, but they also provided polymer-metal crevices for evaluating the effects of this type of crevice simultaneously with metal-metal crevices.

The surfaces of the metal coupons were prepared by surface grinding followed by rinsing in acetone. After assembly, the nuts and bolts were tightened to a torque of 0.56 N-m (80 oz-in.). The crevice assemblies were suspended in one liter vessels immersed in oil baths maintained at 100 C. The kettles were nearly filled with a 50:50 mixture of either ethylene glycol/ASTM water or propylene glycol/ASTM water. The solutions were aerated throughout the exposures. Severity of crevice corrosion was determined by optical microscopy of specimens at the end of each test.

Galvanic Corrosion

The effect of galvanic coupling on corrosion was evaluated in experiments involving a wide variety of bimetallic couples. Equal areas of strip specimens, about 7 cm^2 in exposed area, were etched and inserted through stoppers into polyethylene bottles nearly filled with a 50:50 mixture of either ethylene glycol/ASTM water or propylene glycol/ASTM water. The bottles were immersed in oil baths maintained at 93 C, and the solutions were aerated throughout the exposures. Corrosion potentials,

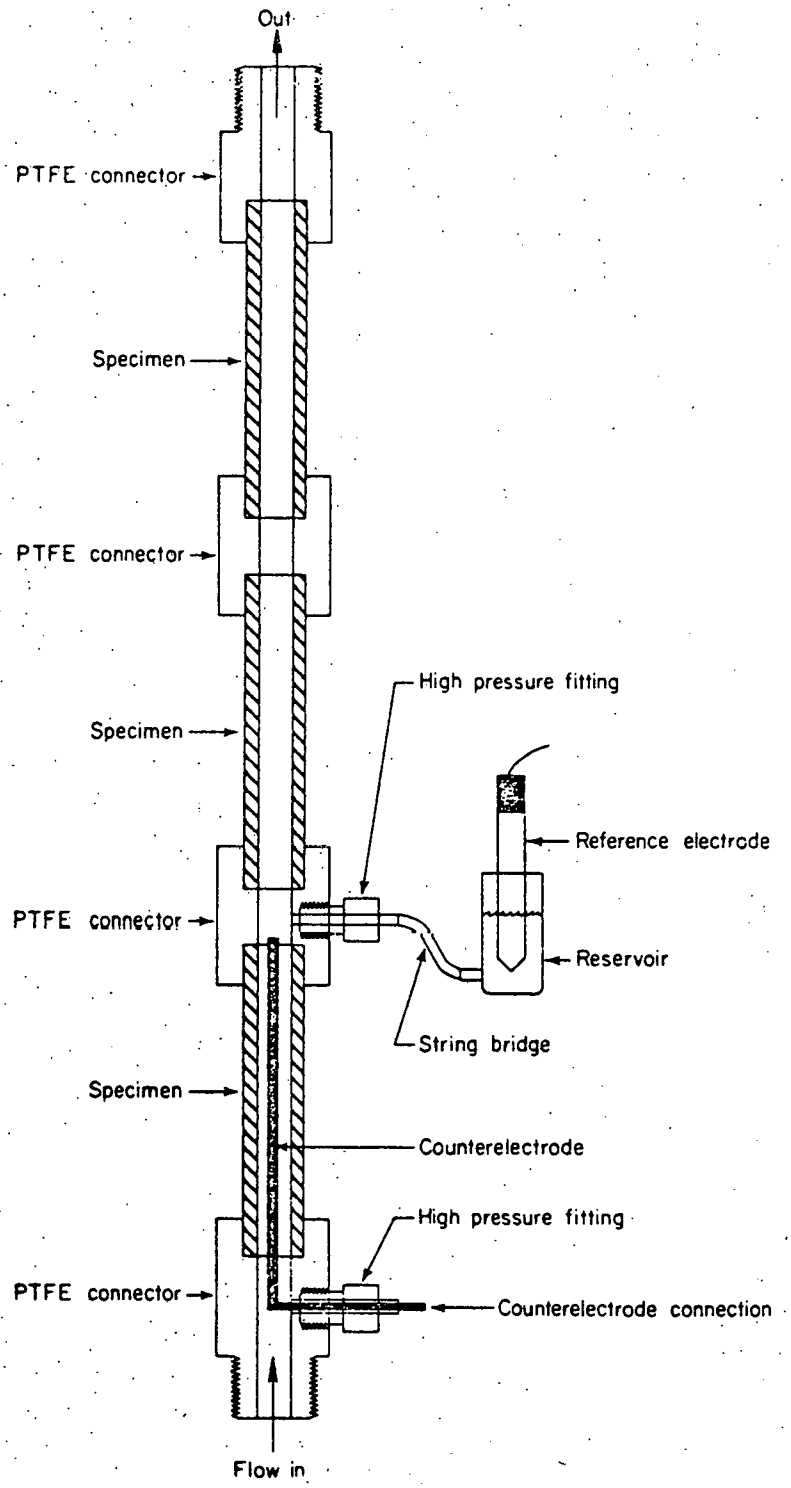

FIGURE 3. SPECIMEN ASSEMBLY

Each assembly consisted of three tubular specimens, PTFE connectors, HC-276 counterelectrode, and reference electrode. Each specimen was surrounded by thermal insulation (not shown)

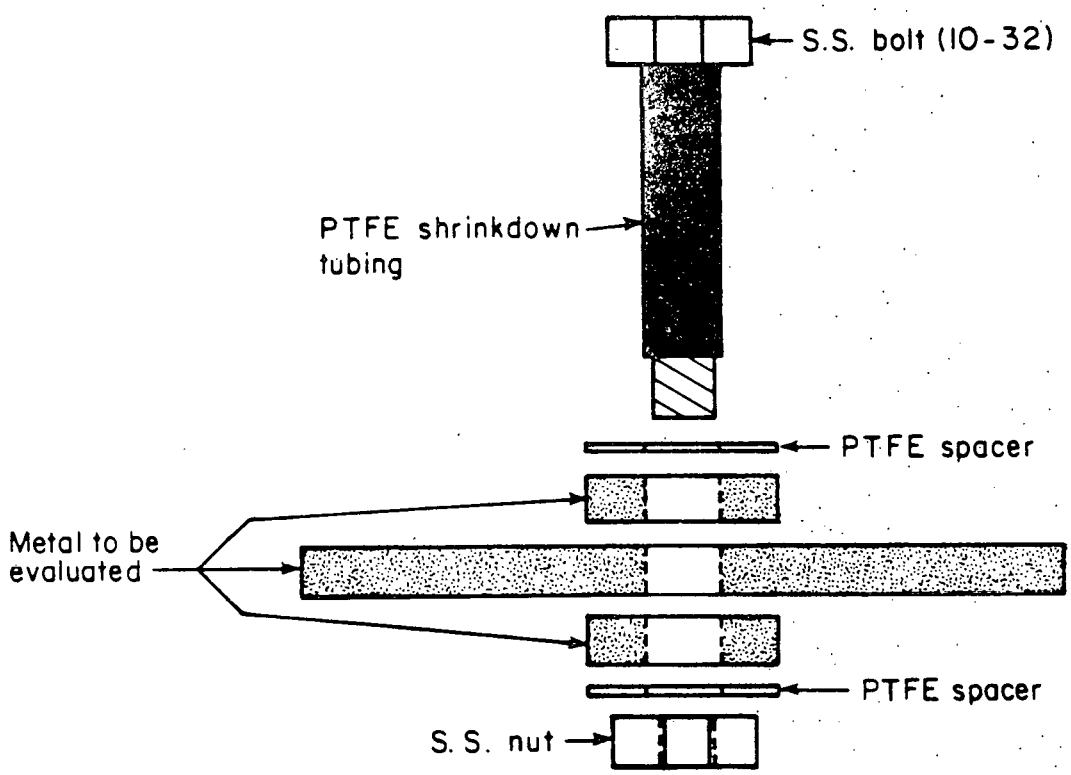

FIGURE 4. ASSEMBLY USED TO EVALUATE CREVICE CORROSION SUSCEPTIBILITY

E_{corr}, of the coupled and uncoupled electrodes were measured periodically by means of a string bridge, SCE, and high impedance electrometer. Galvanic current was monitored intermittently with a zero resistance ammeter. The electrode pairs were electrically shorted to each other throughout the exposure periods.

RESULTS

Corrosion Under Dynamic Flow

A summary of experiments performed in the recirculating system is presented in Table 2. A total of eleven experiments was performed, ranging in duration from 259 to 522 hours. Experiments 9 and 10 incorporated the effects of heat transfer through specimens to the solution. Experiment 11 involved the highest level of chloride used, namely, 100 ppm in the aqueous EG solution. Experiments in PG/ASTM water were not performed because trends could be predicted adequately from analogous experiments in EG/ASTM water.

Solution pH, Polarization Resistance, Corrosion Potential

Variations in solution pH, polarization resistance (PR), and corrosion potential (E_{corr}) are given in Table 3 for EG solutions and in Table 4 for PG solutions.

Considering pH, in EG solutions it decreased with increasing exposure time in all but the EG/ASTM water solution exposed to aluminum alloys. The pH decreases were caused primarily by oxidation of the EG resulting in acidic by-products; similar degradation was observed in Task 3 of this research project[2], and analysis of aqueous glycol solutions after prolonged periods at elevated temperatures confirmed the presence of organic acids, including oxalic acid. The degree of acidification

TABLE 2. SUMMARY OF EXPERIMENTS PERFORMED IN THE RECIRCULATING SYSTEM[a]

Experiment Number	Corrodent[b]	Alloys	Atmosphere	Duration[c], hr
1	EG/ASTM water	Al 1100, 3003, 6061	air or N_2	330
2	EG/ASTM water	copper, steel, stainless steel	air or N_2	522
3	EG/20% ASTM water[d]	Al 1100, 3003, 6061	air or N_2	451
4	EG/20% ASTM water[d]	copper, steel, stainless steel	air or N_2	438
5	PG/20% ASTM water[d]	copper, steel, stainless steel	air or N_2	352
6	PG/20% ASTM water[d]	Al 1100, 3003, 6061	air or N_2	432
7	EG/distilled water	Al 1100, 3003, 6061	air or N_2	309
8	EG/distilled water	copper, stainless steel	air or N_2	351
9[e]	PG/distilled water	Al 1100, 3003, 6061	air or N_2	259
10[e]	PG/distilled water	copper, stainless steel	air or N_2	334
11	EG/high Cl^- water[f]	copper, stainless steel	air or N_2	309

(a) Temperature and flow rate were maintained at 100 C and 61 cm/sec (2 ft/sec), respectively, during each experiment.

(b) EG = ethylene glycol; PG = propylene glycol; ASTM water contained 100 ppm each of Cl, SO_4 and HCO_3 ions (see text). Equivolume mixtures were used.

(c) Total duration; approximately 10 to 20 percent of the total exposure time accrued at temperatures less than 100 C are included in these times.

(d) This was ASTM water diluted 4:1 with distilled water prior to mixing with EG or PG.

(e) These experiments incorporated the effects of heat flow through the tubular specimens to the solution.

(f) The water used to make this equivolume mixture contained 200 ppm Cl, 100 ppm SO_4, and 100 ppm HCO_3.

TABLE 3. VARIATION IN CORROSION-RELATED PARAMETERS FOR SPECIMENS EXPOSED TO ETHYLENE GLYCOL IN THE RECIRCULATING SYSTEM

Experiment Number	Corrodent	Specimen Material	Elapsed Time, hr	Temperature, °C	Atmosphere	Corrosion Potential, V(SCE)	Polarization Resistance, ohm-cm² ×10³	Solution pH
8	EG/distilled water	Copper 122	16	93	air	0.033	2620	5.5
		T444				0.136	4880	
		Copper 122	23	99	air	-0.076	262	5.5
		T444				0.187	394	
		Copper 122	329	99	air	0.194	39	4.7
		T444				0.255	58	
		Copper 122	351	99	N_2	0.185	22	4.6
		T444				0.220	36	
7	EG/distilled water	Al 1100	21	30	air	-0.235	2430	5.7
		Al 3003				-0.290 to -0.309	2340	
		Al 6061				-0.250	469	
		Al 1100	29	100	air	-0.513	806	5.4
		Al 3003				-0.604	347	
		Al 6061				-0.531	450	
		Al 1100	213	100	air	-0.180	262	4.4
		Al 3003				-0.190	193	
		Al 6061				-0.163	262	
		Al 1100	296	100	N_2	-0.277	262	4.1
		Al 3003				-0.305	206	
		Al 6061				-0.245	262	
4	EG/20% ASTM water	Copper 122	20	32	air	0.023	628	7.6
		T444				0.038	22,500	
		1018 steel				-0.300	431	
		Copper 122	29	100	air	-0.044	141	7.5
		T444				-0.046	900	
		1018 Steel				-0.559	86	
		Copper 122	358	100	air	-0.144	6.6	
		T444				-0.159	2.6	
		1018 steel				-0.499	3.0	
		Copper 122	429	100	N_2	-0.269	3.6	4.2
		T444				-0.297	1.7	
		1018 steel				-0.576	1.7	
3	EG/20% ASTM water	Al 1100	3	70	air	-0.526	-	7.6
		Al 3003				-0.850	-	
		Al 6061				-1.050	-	
		Al 1100	23	100	air	-0.856	142	
		Al 3003				-0.916	90	
		Al 6061				-0.925	129	
		Al 1100	358	100	air	-0.130	862	3.8
		Al 3003				-0.145	825	
		Al 6061				-0.171	1290	
		Al 1100	433	100	N_2	-0.173	3000	4.1
		Al 3003				-0.188	1730	
		Al 6061				-0.205	2250	
2	EG/ASTM water	Copper 122	19	22	air	-0.003	126	7.6
		T444				0.021	37,500	
		1018 steel				-0.405	52	
		Copper 122	25	100	air	-0.024	21	9.7
		T444				-0.014	394	
		1018 steel				-0.621	9.0	
		Copper 122	186	100	air	-0.040	28	
		T444				0.033	469	
		1018 steel				-0.450	11	
		Copper 122	426	100	air	-0.087	11	4.5
		T444				0.101	14	
		1018 steel				-0.585	9.9	
		Copper 122	522	100	N_2	-0.147	24	4.5
		T444				-0.045	21	
		1018 steel				-0.603	12.9	
1	EG/ASTM water	Al 1100	18	34	air	-0.522	122	7.6
		Al 3003				-0.564	225	
		Al 6061				-0.542	187	
		Al 1100	41	101	air	-1.09	34	9.1
		Al 3003				-1.00	24	
		Al 6061				-1.03	319	
		Al 1100	186	101	air	-0.943	47	
		Al 3003				-1.00	49	
		Al 6061				-1.00	41	
		Al 1100	234	101	N_2	-0.933	52	8.8
		Al 3003				-1.00	49	
		Al 6061				-0.992	34	
11	EG/ASTM water + 50 ppm Cl	Copper 122	21	33	air	-0.041	161	7.6
		T444				-0.009	262	
		Copper 122	29	100	air	+0.076	49	
		T444				+0.057	206	
		Copper 122	237	100	air	0.104	5.6	4.7
		T444				0.159	4.5	
		Copper	309	100	N_2	0.075	8.1	4.5
		T444				0.107	4.1	

TABLE 4. VARIATION IN CORROSION-RELATED PARAMETERS FOR SPECIMENS EXPOSED TO PROPYLENE GLYCOL IN THE RECIRCULATING SYSTEM

Experiment Number	Corrodent	Specimen Material	Elapsed Time, hr	Temperature, °C	Atmosphere	Corrosion Potential, V(SCE)	Polarization Resistance, ohm-cm^2·10^3	Solution pH
10	PG/distilled water	Copper 122	15	33	air	0.109	1260	4.1
		T444				0.158	3190	
		Copper 122	23	100	air	0.094	109	
		T444				0.183	129	
		Copper 122	257	100	air	0.171	64	4.7
		T444				0.191	92	
		Copper 122	334	100	N_2	0.158	41	4.5
		T444				0.157	56	
9	PG/distilled water	Al 1100	19	34	air	-0.277	1520	4.5
		Al 3003				-0.312	1425	
		Al 6061				-0.142	3750	
		Al 1100	26	99	air	-0.534	206	4.6
		Al 3003				-0.677	187	
		Al 6061				-0.777	225	
		Al 1100	187	99	air	-0.097	600	4.3
		Al 3003				-0.082	544	
		Al 6061				-0.120	675	
		Al 1100	259	99	N_2	-0.111	619	4.2
		Al 3003				-0.104	516	
		Al 6061				-0.135	712	
5	PG/20% ASTM water	Copper 122	16	30	air	0.006	144	4.5
		T444				0.043	675	
		1018 steel				-0.515	165	
		Copper 122	24	100	air	-0.117	28	4.5
		T444				-0.027	32	
		1018 steel				-0.630	16	
		Copper 122	328	100	air	-0.159	9.7	4.2
		T444				-0.131	6.0	
		1018 steel				-0.570	6.6	
		Copper 122	352	100	N_2	-0.297	5.8	4.6
		T444				-0.298	3.4	
		1018 steel				-0.598	4.7	
6	PG/20% ASTM water	Al 1100	16	29	air	-0.343	450	4.1
		Al 3003				-0.457	506	
		Al 6061				-0.417	600	
		Al 1100	23	100	air	-0.751	67	4.1
		Al 3003				-0.679	90	
		Al 6061				-0.762	101	
		Al 1100	352	100	air	-0.203	127	4.4
		Al 3003				-0.205	184	
		Al 6061				-0.196	206	
		Al 1100	424	100	N_2	-0.510	165	4.4
		Al 3003				-0.463	216	
		Al 6061				-0.482	244	

was fairly uniform among the experiments (except Number 1), ranging between about 4 and 5 units after 230 to 520 hours of circulation. Similar pH shifts were not observed in the PG solutions, probably because of the relatively low initial pH of these solutions.

Concerning E_{corr}, that of copper 122 shifted in the noble direction with increasing exposure time in EG/distilled water and in EG/ASTM water plus 50 ppm Cl. It moved in the active direction in EG/20% ASTM water and EG/ASTM water. Qualitatively similar behavior was observed in PG/distilled water and PG/20% ASTM water. E_{corr} of T444 stainless steel moved in the noble direction in EG/distilled water, PG/distilled water, EG/20% ASTM water and EG/ASTM water in equilibrium with air; deaeration usually caused a large active shift. In PG/20% ASTM water the shift was in the active direction regardless of the atmosphere in equilibrium with the solution. E_{corr} of the 1018 steel was relatively active for all exposure conditions, as expected, and it was not largely influenced by changes in solution chemistry. E_{corr} of the aluminum alloys displayed the greatest relative movements. For example, the respective final potentials of 1100, 3003, and 6061 alloys were -0.277, -0.305, and -0.245 V(SCE) in EG/distilled water, but they were -0.933, -1.00, and -0.992 V(SCE), respectively, in EG/ASTM water. Similar changes in the active direction were observed for these three alloys in PG/20% ASTM water, relative to those in PG/distilled water. Potential behavior during a given experiment was less definable. Thus, in EG/distilled water E_{corr} of the three aluminum alloys exhibited maxima (i.e., were most noble) part way through the exposure, whereas in EG/ASTM water the values essentially shifted monotonically in the active direction. It will be shown in a subsequent section that corrosion potential correlated qualitatively with pitting behavior for the aluminum-base alloys.

Polarization resistance measurements were made periodically to ascertain, in a semi-quantitative manner, real-time corrosion behavior of specimens in the recirculating system. Polarization resistance provides

a measure of the instantaneous corrosion rate of an electrode provided certain system parameters are known. Specifically, the Stearn-Geary equation states that the corrosion current, i_c, at an electrode under activation control is given by the equation,

$$i_c = \frac{1}{2.3} \frac{\beta_a \beta_c}{\beta_a + \beta_c} \frac{i_{app}}{\Delta E}, \qquad (1)$$

in which β_a and β_c are anodic and cathodic Tafel constants, and i_{app} is the current measured when the electrode is polarized from its freely corroding potential by a polarizing voltage of magnitude ΔE. The applied polarization, ΔE, is typically 5 to 15 millivolts. The slope of a curve of applied voltage, ΔE, versus current, i_{app}, has units of volts/ampere, or ohms, and therefore is referred to as the polarization resistance, PR. Examination of Equation 1 shows that, for constant values of β_a and β_c, corrosion rate (i_c) is inversely proportional to PR, which is $\Delta E/i_{app}$. Thus, a fluctuation of PR of a corroding electrode to a larger value indicates a reduction in corrosion rate. If it is assumed that β_a and β_c are relatively constant throughout an experiment (which is almost never strictly true, but which often provides sufficient accuracy for detecting the effects of major variables), these variations in PR can be used to estimate the influences of experimental variables on corrosion rate. The PR data could not be transformed into actual instantaneous corrosion rates for two reasons. First, the Tafel slopes necessary to reduce the PR data could not be measured with sufficient accuracy because of IR drop effects in the solution. Second, it appears that redox reactions were occurring in the glycol solutions simultaneously with corrosion, and such reactions possibly would have introduced errors into the calculated corrosion rates. Therefore relative changes in PR were used to ascertain the influence of experimental variables on corrosion rate.

An indication of PR-time behavior is given in Tables 3 and 4. Usually, a large reduction of PR occurred during initial heating of the electrolyte, whereas subsequent behavior depended on the corrosivity of the particular electrolyte. By way of illustration, PR-time behavior is presented in Figures 5 through 11 for selected experiments.

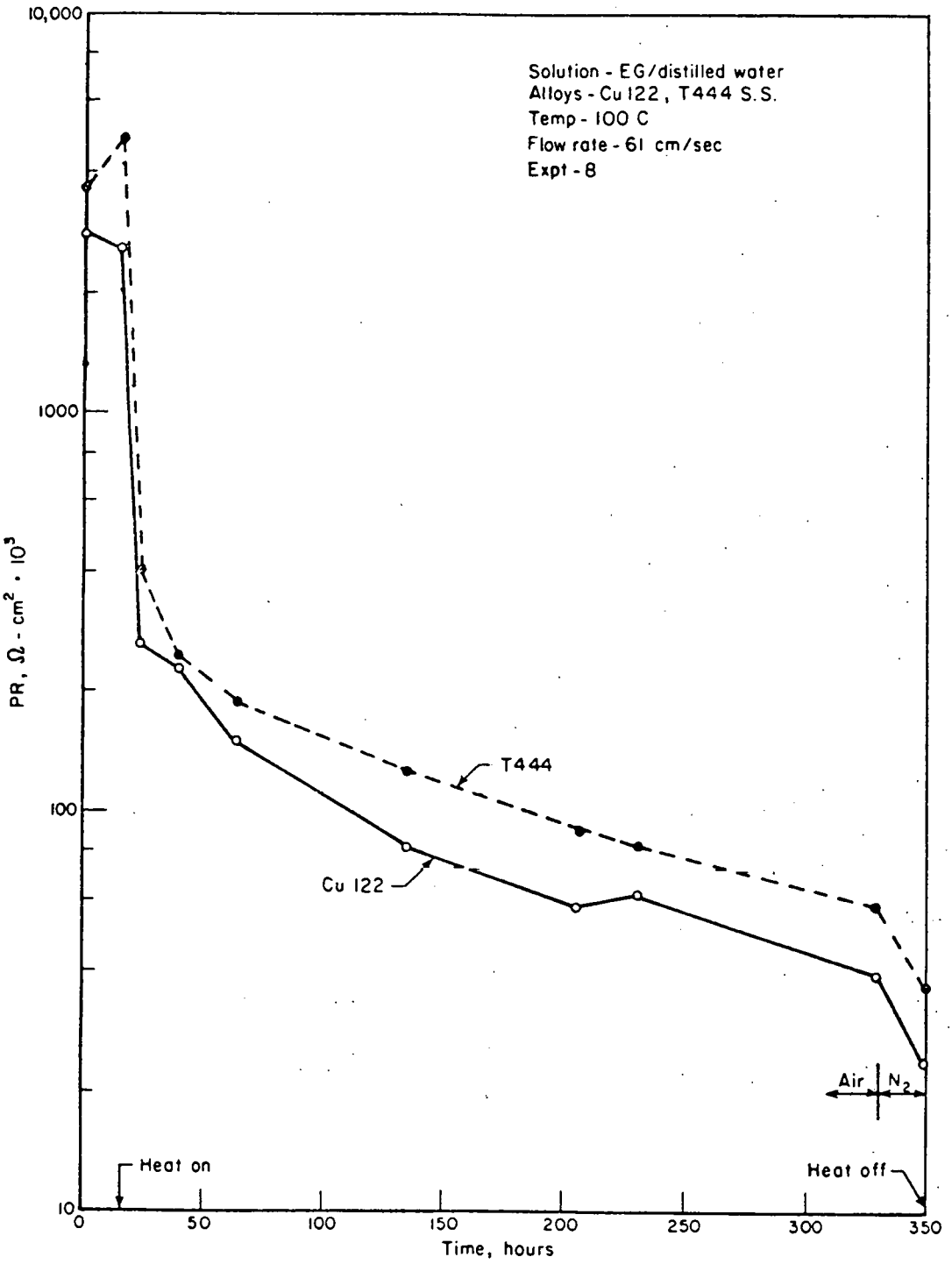

FIGURE 5. PR VERSUS TIME FOR Cu 122 AND T444 STAINLESS STEEL IN EG/DISTILLED WATER

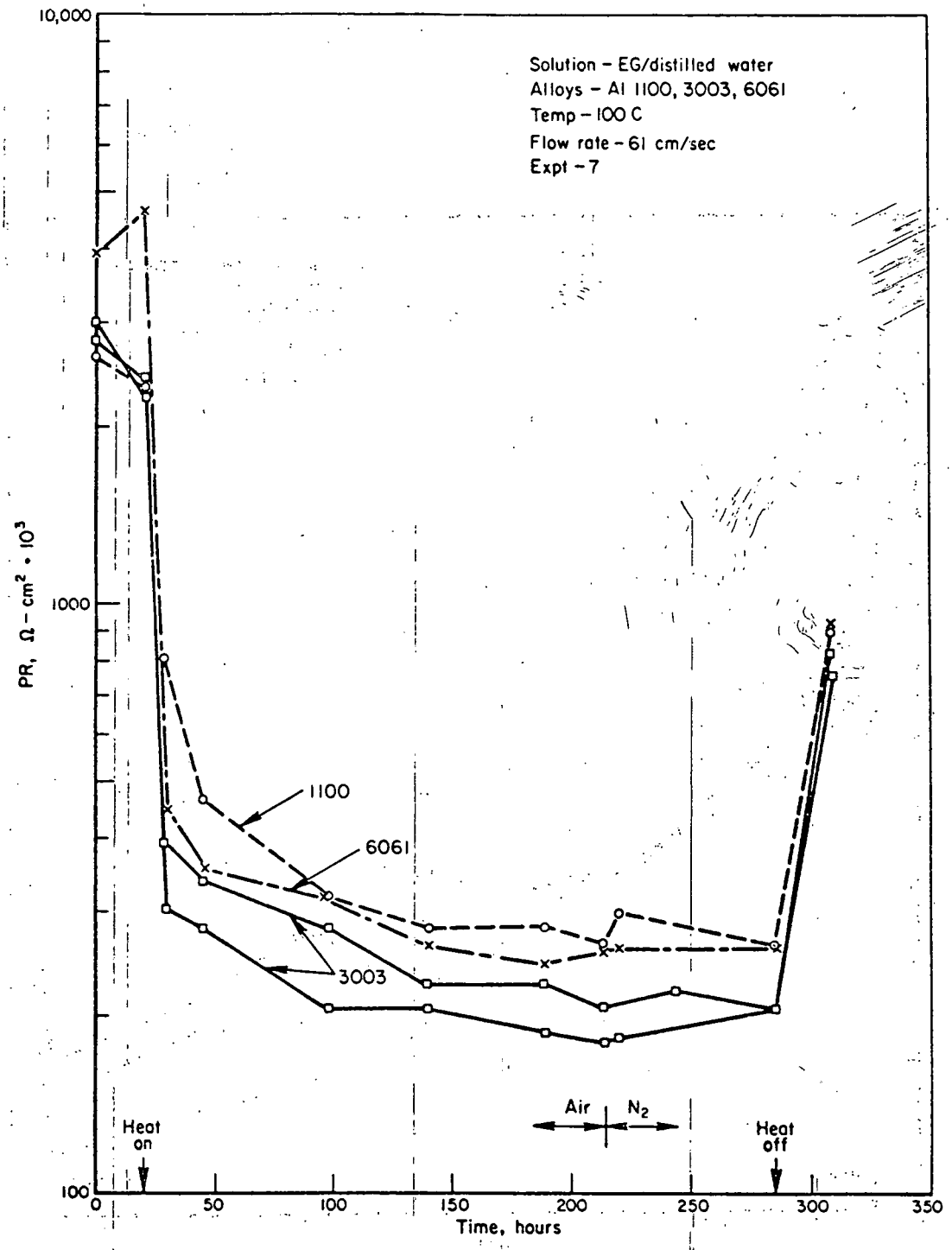

FIGURE 6. PR VERSUS TIME FOR Al ALLOYS 1100, 3003, AND 6061 IN EG/DISTILLED WATER

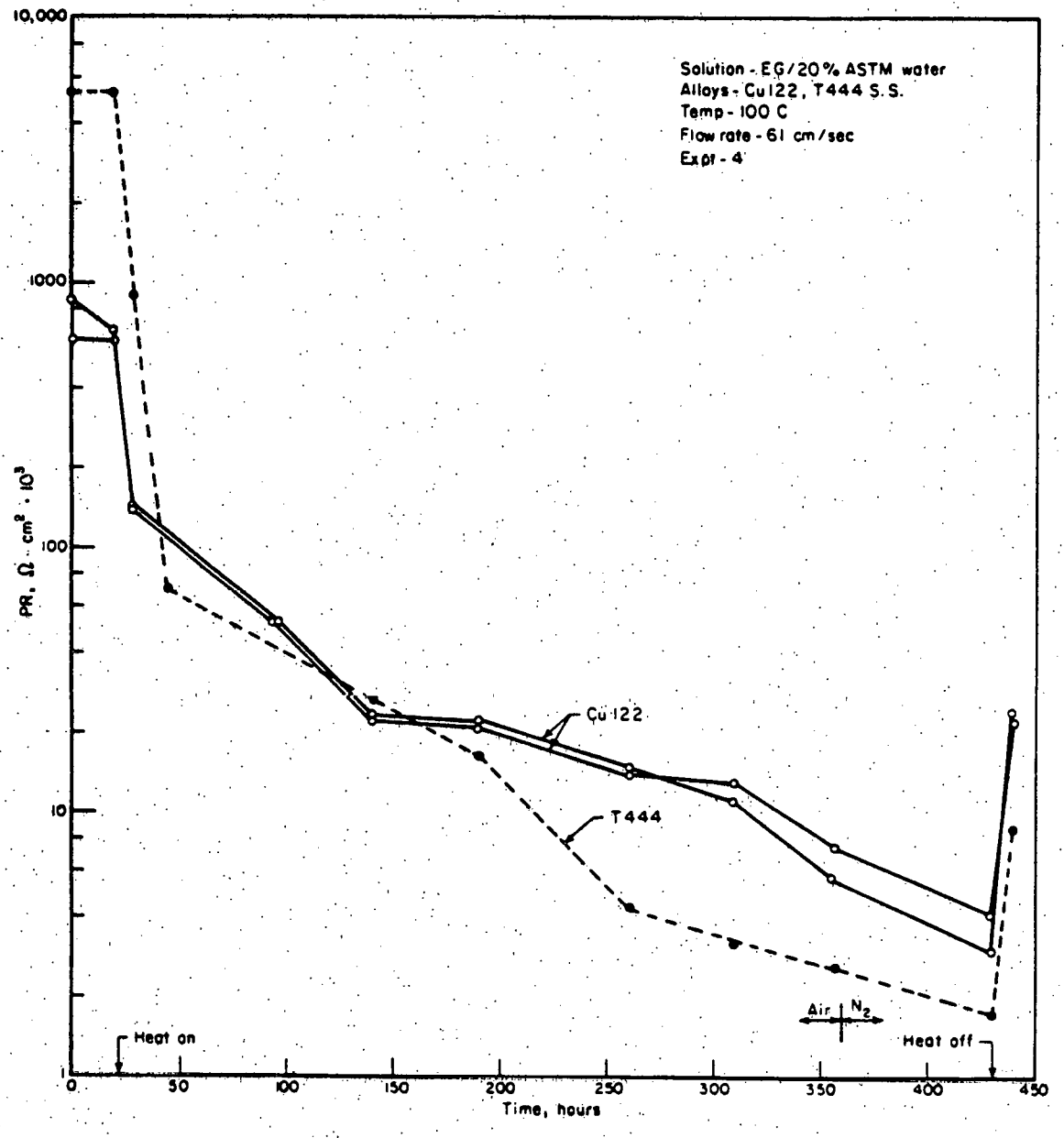

FIGURE 7. PR VERSUS TIME FOR Cu 122 AND T444 STAINLESS STEEL IN EG/20% ASTM WATER

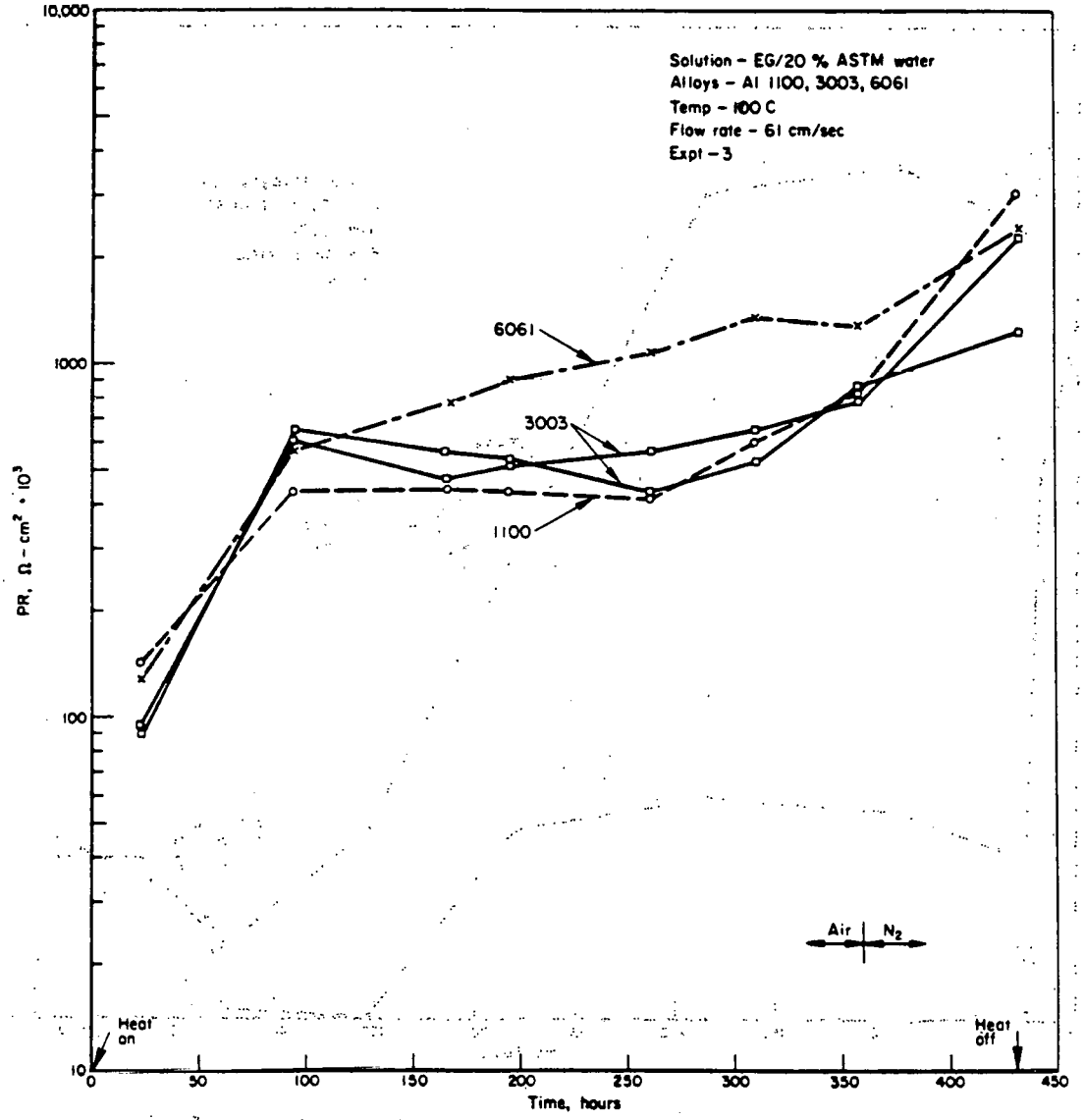

FIGURE 8. PR VERSUS TIME FOR Al ALLOYS 1100, 3003, AND 6061 IN EG/20% ASTM WATER

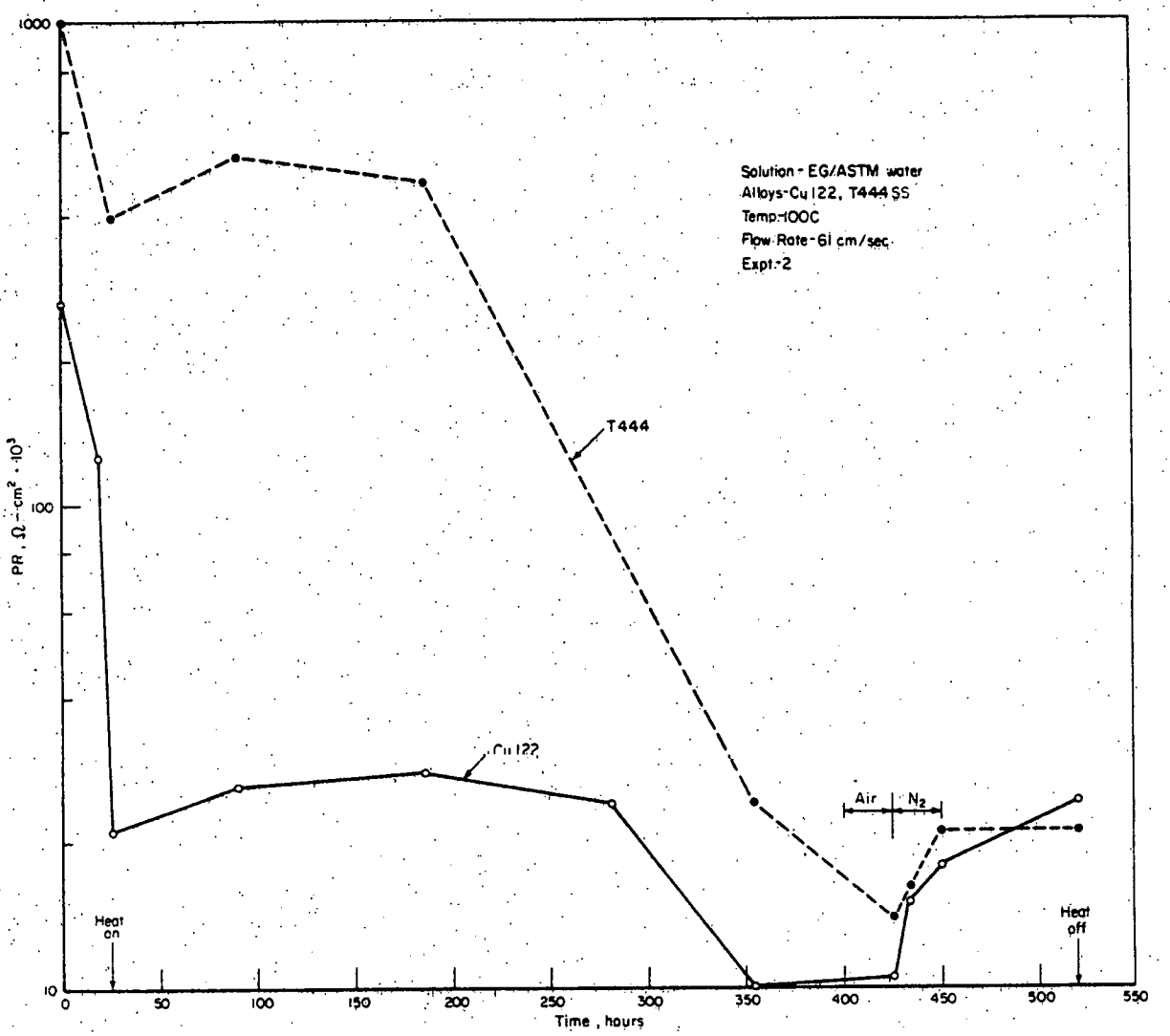

FIGURE 9. PR VERSUS TIME FOR Cu 122 and T444 STAINLESS STEEL IN EG/ASTM WATER

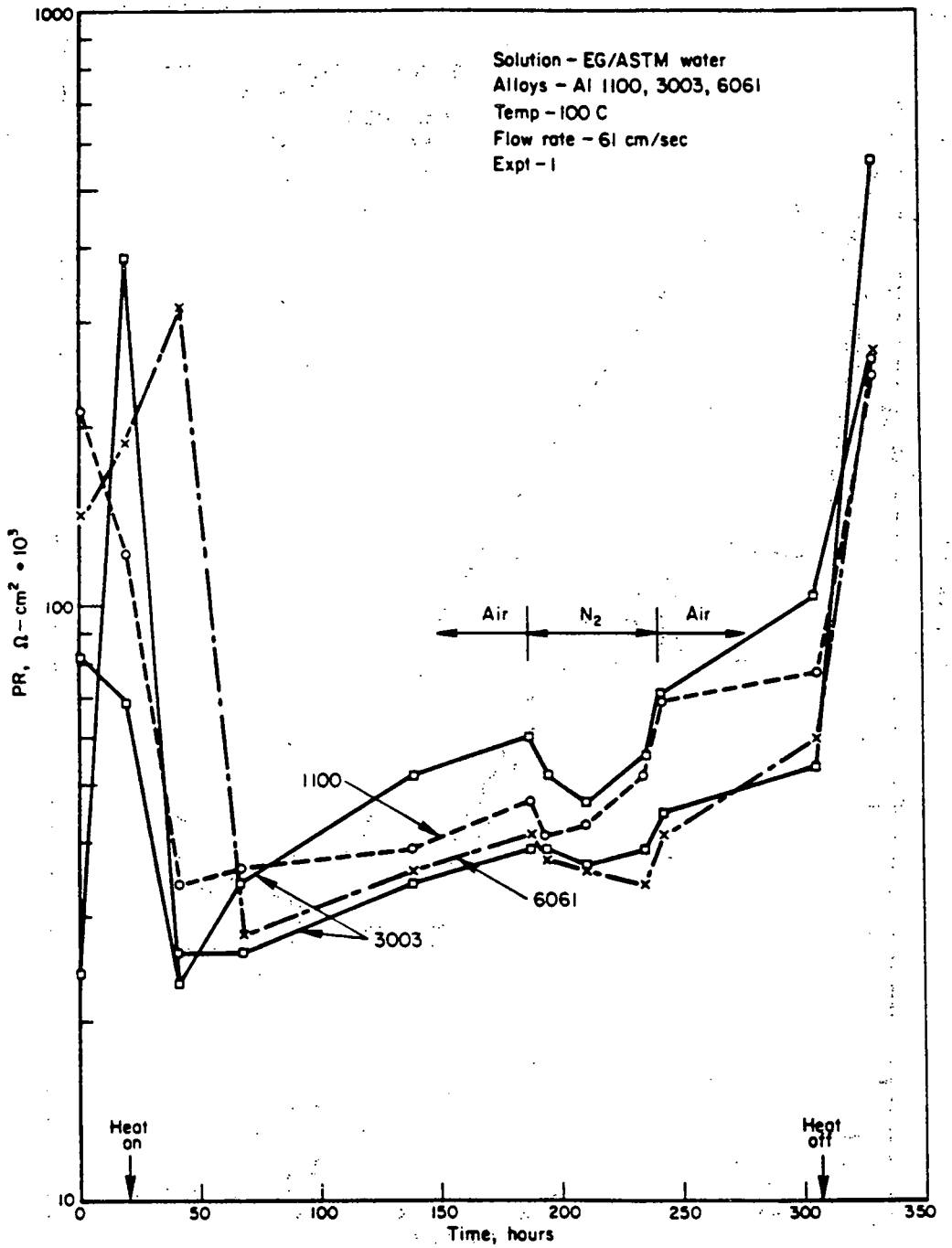

FIGURE 10. PR VERSUS TIME FOR Al ALLOYS 1100, 3003, AND 6061 IN EG/ASTM WATER

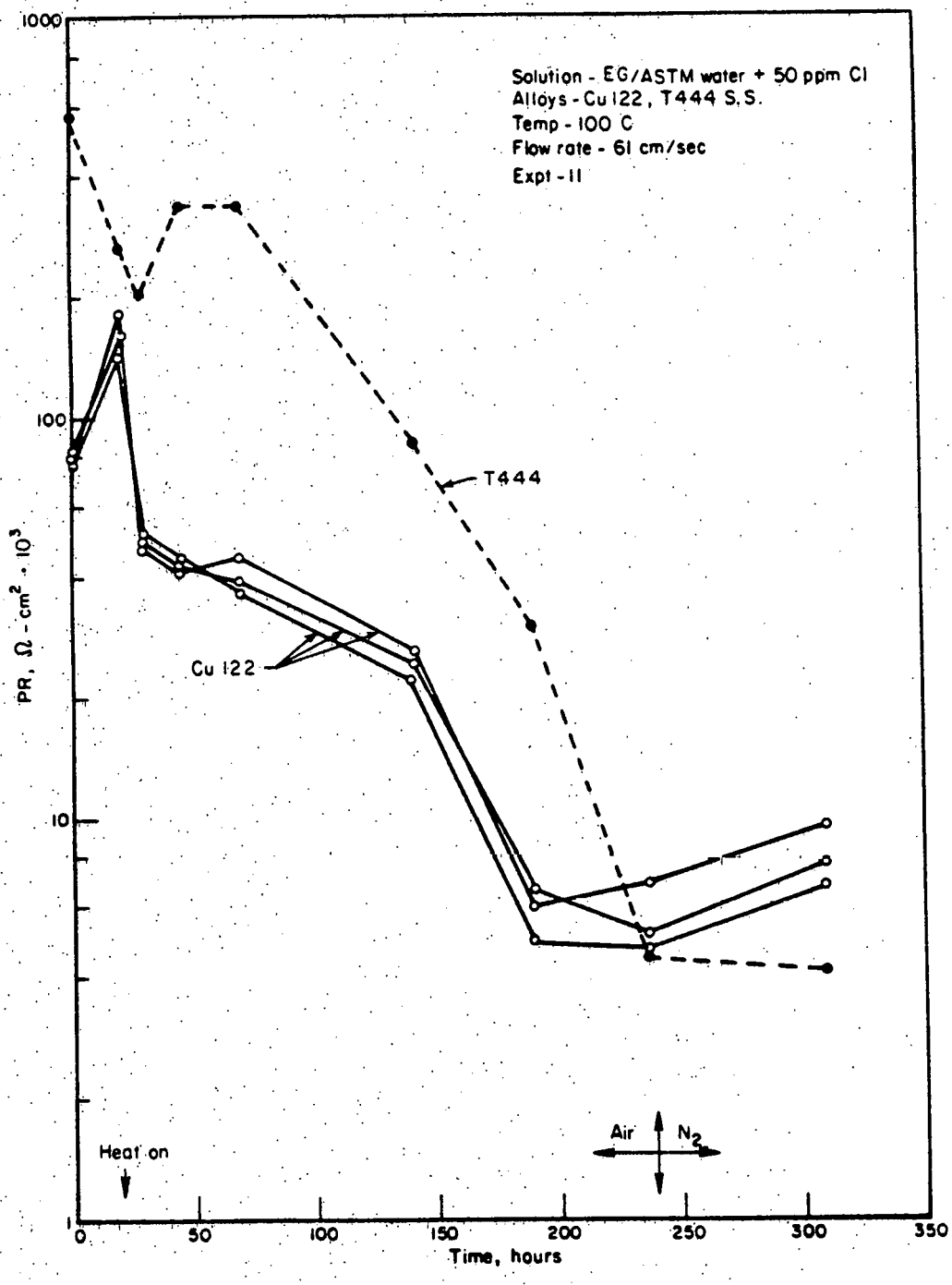

FIGURE 11. PR VERSUS TIME FOR Cu 122 AND T444 STAINLESS STEEL IN EG/ASTM WATER + 50 ppm Cl

Several features of Figures 5 to 11 are noteworthy. First, the PR decreased markedly, often by several orders of magnitude, when the EG solutions were heated to 100 C from time 0, at which the temperature was about 30 C. This behavior was expected due to the thermally activated nature of corrosion and electrochemical reactions in general. This decrease also presumably occurred in Figure 8, but it was not resolved because no PR measurements were taken at ambient temperature, i.e., at time t = 0. Figures 5, 6, and 11 indicate that a steady state condition had been reasonably well established by the end of the exposure to air, that is, prior to substitution of N_2 for the air atmosphere above the recirculating solution. However, Figures 8 to 10 show that steady state had not been established. Specifically, in Experiment 1 and 3, Figures 10 and 8, the PR was slowly increasing, indicating a slow reduction in corrosion rate with increasing exposure time. In Experiment 2, Figure 9, the apparent corrosion rate was still increasing.

It should not be assumed that corrosion represents the only oxidation reaction giving rise to the PR behavior shown in these figures. Corrosion data from T444 will be presented that indicates that other redox reactions apparently occurred in conjunction with corrosion, because although the low PR values observed on T444 stainless steel suggest a rapid corrosion rate, no measurable corrosion was detected on this alloy under any exposure conditions.

Toward the end of each experiment nitrogen was substituted for air in contact with the solution to determine the effect of atmospheric oxygen on PR and E_{corr}. In Figures 5, 6, 7, and 11 no effect of removing atmospheric oxygen was observed. Figures 8 and 9 show an increase in PR upon substitution of nitrogen, indicating a reduction in overall oxidation rate with oxygen removal. Figure 10 shows an opposite effect, namely, a slight enhancement of oxidation rate with oxygen removal and restoration of this rate upon its re-introduction.

Corrosion Rates

Corrosion rate data based on weight loss are presented in Tables 5 and 6. No pitting occurred on copper 122, and on T444 and 1018 steels. Because

TABLE 5. AVERAGE CORROSION RATES FOR COPPER, STAINLESS STEEL, AND PLAIN CARBON STEEL OBTAINED IN THE RECIRCULATING SYSTEM

Experiment Number	Corrodent	Alloy	Average Corrosion rate[(a)]	
			$mg/cm^2/yr$	μm/yr
8	EG/distilled water	Copper 122	152	171
		T444 SS	<1	<1
4	EG/20% ASTM water	Copper 122	90	101
		T444 SS	<1	<1
		1018 steel	3930	5040
2	EG/ASTM water	Copper 122	160	180
		T444 SS	<1	<1
		1018 steel	890	1140
11	EG/ASTM water + 50 ppm Cl	Copper 122	212	239
		T444 SS	<1	<1
10	PG/distilled water	Copper 122	71	80
		T444 SS	<1	<1
5	PG/20% ASTM water	Copper 122	70	79
		T444 SS	<1	<1
		1018 steel	2930	3760

(a) Rates are averages from triplicate tube specimens. They were extrapolated to annual rates in a linear manner.

TABLE 6. MAXIMUM PIT DEPTHS AND APPROXIMATE PIT DENSITIES FOR ALUMINUM ALLOYS EXPOSED IN THE RECIRCULATING SYSTEM

Experiment Number	Corrodent	Alloy	Exposure Time,(a) hr	Maximum Pit Depth,(b) μm	Maximum Pit Density, cm^{-2}
7	EG/distilled water	1100	260	5	$>1.8 \cdot 10^5$
		3003		5	$< 9 \cdot 10^3$
		6061		19	$>1.8 \cdot 10^5$
3	EG/20% ASTM water	1100	440	6	$>1.8 \cdot 10^5$
		3003		8	$>1.8 \cdot 10^5$
		6061		20	$>1.8 \cdot 10^5$
1	EG/ASTM water	1100	285	72	$>1.8 \cdot 10^5$
		3003		127	$>1.8 \cdot 10^5$
		6061		150	$>1.8 \cdot 10^5$
9	PG/distilled water	1100	234	3	$< 9 \cdot 10^3$
		3003		4	$< 9 \cdot 10^3$
		6061		13	$>1.8 \cdot 10^5$
6	PG/20% ASTM water	1100	404	3	$>1.8 \cdot 10^5$
		3003		5	$< 9 \cdot 10^3$
		6061		14	$>1.8 \cdot 10^5$

(a) Time at operating temperature, 100 C.

(b) Determined by means of a microscope with a calibrated focus adjustment. Pit depths and pit densities were obtained by examining about 125 cm^2 of each type of specimen.

pitting was the predominant form of attack on all three aluminum alloys, corrosion data are presented as a rate of pitting rather than a rate of overall weight loss in Table 6. The corrosion rates of copper in EG solutions were least in EG/20% ASTM water (101 μm/yr) and greatest in EG/ASTM water plus 50 ppm chloride (239 μm/yr). Intermediate rates occurred in EG/distilled water (171 μm/yr) and EG/ASTM water (180 μm/yr). These rates are approximate because they are extrapolated to an annual basis, a period about 25 times longer than the exposure times. Furthermore, there may have been some protection afforded by a growing corrosion product film, although such films were not well developed on the copper tube specimens after exposure. These corrosion rates provide an estimate of the upper bound of the rate of attack, and they are adequate for assessing the suitability of an alloy/solution combination over a 10 to 20 year design lifetime. Since the wall thickness was 889 μm (0.035 in.), a corrosion rate of 89 μm/yr would penetrate a tube in 10 years.

The corrosion rate of T444 stainless steel was less than 1 μm/yr under every exposure condition studied. The high concentrations of chromium and molybdenum resulted in an extremely protective passive film that was almost totally inert in the various test solutions. The corrosion rates of 1018 steel specimens were relatively large, as expected, and ranged between about 1100 to 5000 μm/yr.

In PG solutions the corrosion rate of copper was less than in EG solutions, provided the make-up water was either distilled or 20 percent ASTM water. The corrosion of 1018 steel likewise was less in PG solutions, whereas T444 stainless steel again was unattacked. The difference in corrosivity of PG versus EG solutions was about a factor of two or less.

Pit depths and pit densities are listed in Table 6 for the three aluminum alloys that were investigated. (Because pits in aluminum usually grow at a non-linear rate, some manipulation was required to convert the pit depths into rates of attack; see Table 7). The least susceptible alloy to pitting was 1100 and the most susceptible was 6061. This relationship prevailed in both EG and PG solutions. Except in EG/ASTM water, pitting behavior

of the 3003 alloy more closely approximated that of 1100 aluminum than that of 6061 alloy. Pit depths were somewhat less in PG solutions than in EG solutions. With few exceptions, notably on 3003 alloy, the number of pits per unit area of exposed specimen surface ("pit density") was extremely high, exceeding 1.8×10^{5} cm^{-2}. It is apparent that the mode of attack was one of formation of a great many pits, but relatively shallow in depth.

Pitting rates were calculated in the following manner. Pitting propagation in aluminum has been observed to follow a cube root law[3],

$$D = kt^{1/3}, \qquad (1)$$

where D is measured pit depth, t is exposure time, and k is the pit growth constant. Insertion of the maximum pit depths, D, from Table 6 together with corresponding exposure times, t, into Equation 1 yielded the k values presented in Table 7. These k values were determined from an examination of about 125 cm^2 of specimen surface area; because pitting is statistical by nature, larger specimens might have yielded somewhat deeper pits. Also included in Table 7 are the times, calculated from Equation 1, required to penetrate 889 μm and 508 μm (0.035 in. and 0.020 in.) thick specimens. These thicknesses are in the range that would be encountered in commercial solar collectors, and the penetration times provide an estimate of the useful lifetime of a typical system in the absence of other accelerating influences. Note that penetration would be fastest in EG/ASTM water, where estimated penetration would occur in as little as 1.3 year. In all other environments, calculated penetrations would occur only after long exposure times of the order of 820 to 1,200,000 years. Differences in chloride ion concentration are primarily responsible for this variability.

Effect of Heat Transfer

The influence of heat transfer through the copper and aluminum alloy tube specimens into the circulating solutions is summarized in Tables 8 and 9. The purpose of these experiments was to determine whether effects of heat transfer on corrosion could be neglected without incurring serious error in measurement of corrosion rates. These tables show that neither

TABLE 7. PITTING CONSTANT AND EXTRAPOLATED PIT DEPTHS FOR ALUMINUM ALLOYS EXPOSED IN THE RECIRCULATING SYSTEM

Experiment Number	Corrodent	Alloy	Pitting Constant, k ($\mu m/hr^{1/3}$)	Time Required for Pit Depths of 889 μm and 508 μm, yr[a]	
				889 μm	508 μm
7	EG/distilled water	1100	0.784	$1.7 \cdot 10^5$	$3.1 \cdot 10^4$
		3003	0.784	$1.7 \cdot 10^5$	$3.1 \cdot 10^4$
		6061	2.98	$3.0 \cdot 10^3$	$5.7 \cdot 10^2$
3	EG/20% ASTM water	1100	0.789	$1.6 \cdot 10^5$	$3.1 \cdot 10^4$
		3003	1.05	$6.9 \cdot 10^4$	$1.3 \cdot 10^4$
		6061	2.63	$4.4 \cdot 10^3$	$8.2 \cdot 10^2$
1	EG/ASTM water	1100	10.9	$6.2 \cdot 10^1$	$1.2 \cdot 10^1$
		3003	19.3	$1.1 \cdot 10^1$	$2.1 \cdot 10^0$
		6061	22.8	$6.8 \cdot 10^0$	$1.3 \cdot 10^0$
9	PG/distilled water	1100	0.487	$6.9 \cdot 10^5$	$1.3 \cdot 10^5$
		3003	0.648	$2.9 \cdot 10^4$	$5.5 \cdot 10^4$
		6061	2.11	$8.5 \cdot 10^3$	$1.6 \cdot 10^3$
6	PG/20% ASTM water	1100	0.406	$1.2 \cdot 10^6$	$2.2 \cdot 10^5$
		3003	0.676	$2.6 \cdot 10^5$	$4.8 \cdot 10^4$
		6061	1.89	$1.2 \cdot 10^4$	$2.2 \cdot 10^3$

(a) 889 μm and 508 μm correspond to thicknesses of 0.035 and 0.020 in., respectively.

TABLE 8. INFLUENCE OF HEAT FLUX ON ELECTROCHEMICAL BEHAVIOR OF ALLOY SPECIMENS EXPOSED TO A 50:50 MIXTURE OF PROPYLENE GLYCOL AND DISTILLED WATER AT 100 C[a]

Experiment Number	Specimen Material	Heat Flux[b], W/m^2	Elapsed Time, hr	Atmosphere	Corrosion Potential, V(SCE)	Polarization Resistance, $ohms/cm^2$
10	copper 122	0	23	air	0.094	58
	copper 122	946			0.085	65
	copper 122	4731			0.097	--
	copper 122	0	257	air	0.162	29
	copper 122	946			0.175	38
	copper 122	4731			0.175	--
	copper 122	0	334	N_2	0.156	19
	copper 122	946			0.172	24
	copper 122	4731			0.175	--
9	Al 3003	0	26	air	-0.677	100
	Al 3003	946			-0.695	100
	Al 3003	4731			-0.705	--
	Al 3003	0	187	air	-0.082	290
	Al 3003	946			-0.093	260
	Al 3003	4731			-0.097	--
	Al 3003	0	259	N_2	-0.104	270
	Al 3003	946			-0.105	280
	Al 3003	4731			-0.103	--

(a) Experiments performed in recirculating system at flux rate of 61 cm/sec (RE = 5910)

(b) A heat flux of 946 W/m^2 is equivalent to 300 $BTU/ft^2/hr$, a reasonable upper limit for "the solar power on a surface normal to the sun per unit of collector area a mean distance from earth to sun" (from Applied Solar Energy by Meinel and Meinel, Addison Wesley, Massachusetts (1976), pp 40-41). The value of 4731 W/m^2 was selected because it is five times greater than the maximum solar flux, and about that which occurs in tube and fin collectors.

TABLE 9. INFLUENCE OF HEAT TRANSFER ON CORROSION BEHAVIOR OF ALLOY SPECIMENS EXPOSED TO A 50:50 MIXTURE OF PROPYLENE GLYCOL AND DISTILLED WATER AT 100 C[a]

Experiment Number	Specimen Material	Heat Flux, W/m^2	Maximum Pit Depth, μm	Weight Loss, mg/cm^2
10	Copper 122	0	No pits	2.98[b]
	Copper 122	946	No pits	2.96[c]
	Copper 122	4730	No pits	3.00[d]
9	Al 3003	0	4	0.11[b]
	Al 3003	946	4	0.11[c]
	Al 3003	4730	3	0.09[d]

(a) Experiments performed in recirculating system at a flow rate of 61 cm/sec (N_{Re} = 5910).

(b), (c), (d) Averages from 6, 2, and 1 specimen, respectively.

pitting nor weight loss was influenced substantially by the presence of heat transfer rates up to 4730 W/m^2.

Crevice Corrosion

Results of the crevice corrosion experiments are presented in Table 10, and in selected photographs in Figures 12 through 15. No attack was noted on copper 122 or T444 stainless steel in either EG or PG solutions. Some discoloration did occur in the crevice on T444, and evidence of rather severe general corrosion was found on the freely exposed surfaces of copper 122. Crevice attack on the aluminum alloys, when it occurred, tended to be worse at PTFE-metal interfaces than at metal-metal interfaces, although more experiments need to be performed to strengthen this observation. Crevice corrosion was somewhat less severe in PG/ASTM water, although more experiments are needed to confirm this finding.

Galvanic Coupling

Table 11 summarizes results of galvanic coupling measurements of various electrode pairs. Couples yielding the largest currents, which were proportional to corrosion rates, were those between T444 stainless steel and 1018 steel; fairly large currents also flowed between T444 and copper 122. Currents were least among the aluminum-to-aluminum couples. The influence of type of glycol on the nature of galvanic corrosion was, in some cases, quite pronounced. For example, PG caused a reversal in polarity of couples involving 1100/3003, 3003/6061, and 1018/6061. It also caused much lower currents for couples of 3003/1100, 1018/1100, 1018/3003, 1018/6061, and 444/1018. Variations of uncoupled corrosion potential and galvanic current with exposure time in aerated EG/ASTM water and PG/ASTM water are given in the Appendix.

TABLE 10. SUMMARY OF RESULTS OF CREVICE CORROSION EXPERIMENTS[a]

Solution	Alloy	Severity of Crevice Attack[b]	
		Metal-metal interface	Metal-PTFE interface
EG/ASTM water	1100	Moderate	Minor
	3003	minor	none
	6061	minor	severe
	Cu 122	none	none
	T444	none	none
PG/ASTM water	1100	None	Moderate
	3003	none	minor
	6061	minor	severe
	Cu 122	none	none
	T444	none	none

(a) Duplicate specimens were exposed in non-flowing, aerated solutions at 100 C for 50 days. Chloride concentration was 50 ppm.

(b) Terms are relative.

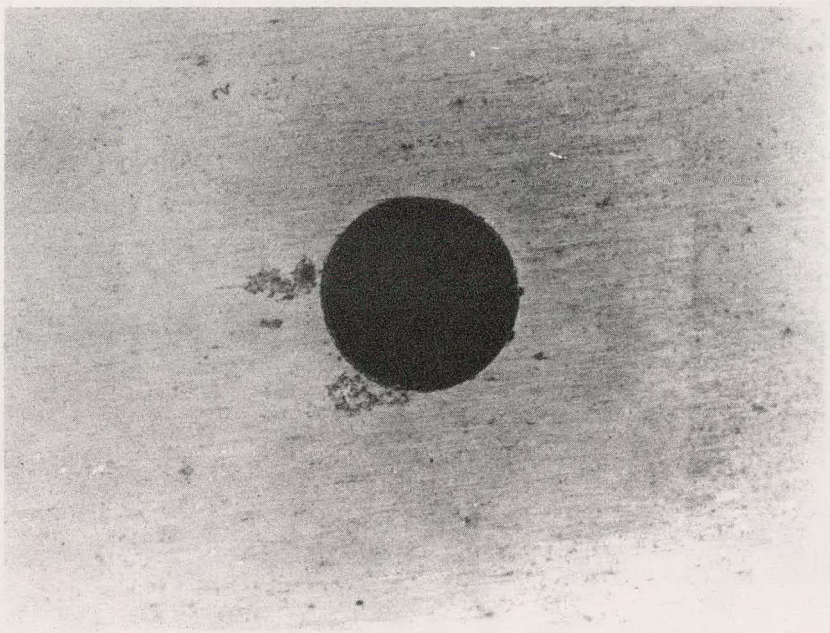

10X

FIGURE 12. MODERATE CREVICE CORROSION ON Al 1100 (METAL-METAL INTERFACE) EXPOSED FOR 50 DAYS IN EG/ASTM WATER AT 100 C

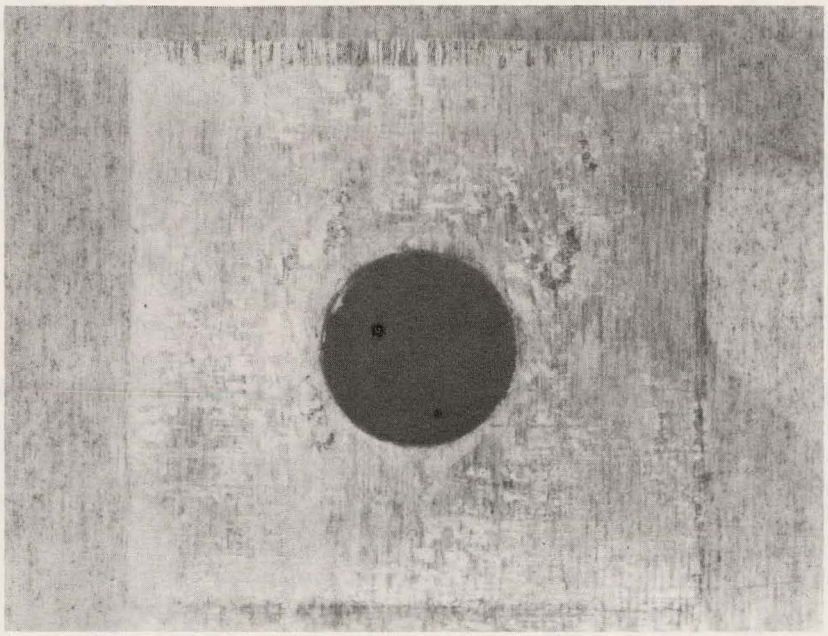

10X

FIGURE 13. MINOR CREVICE CORROSION ON Al 6061 (METAL-METAL INTERFACE) EXPOSED FOR 50 DAYS IN EG/ASTM WATER

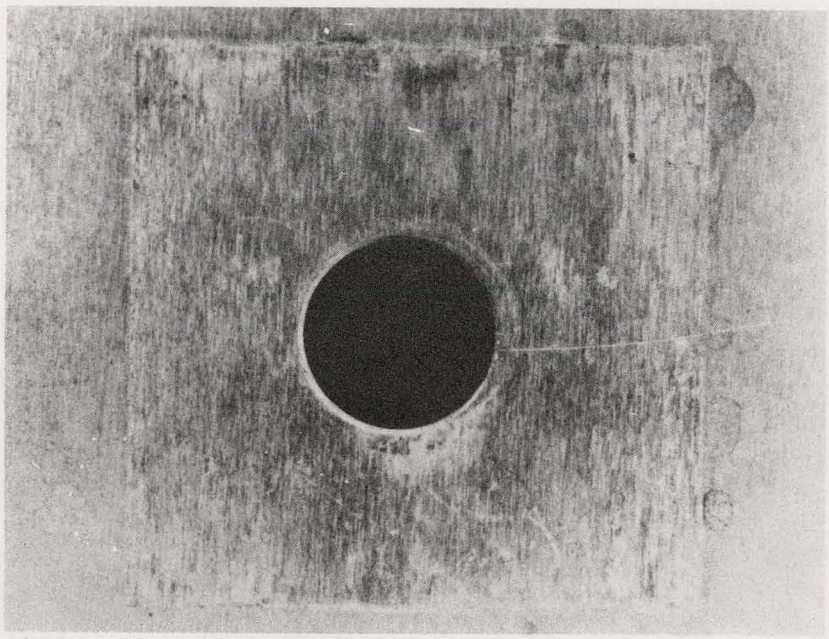

10X

FIGURE 14. SLIGHT CREVICE CORROSION ON Al 6061 (METAL-METAL INTERFACE, NEAR UPPER LEFT HAND CORNER OF CREVICE REGION) EXPOSED FOR 50 DAYS IN PG/ASTM WATER

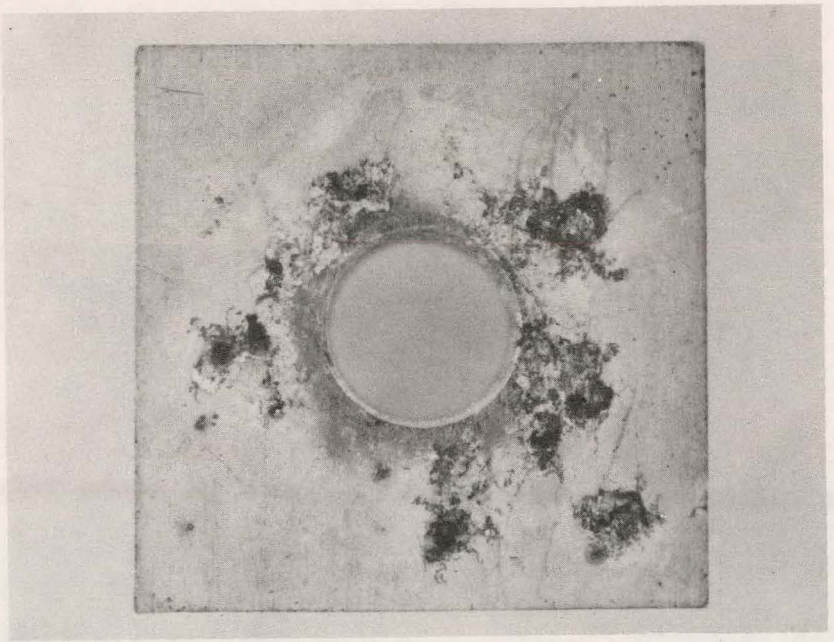

10X

FIGURE 15. SEVERE CREVICE CORROSION ON Al 6061 (PTFE-METAL INTERFACE) EXPOSED FOR 50 DAYS IN EG/ASTM WATER

TABLE 11. RESULTS OF GALVANIC CURRENT EXPERIMENTS IN AERATED EG/ASTM WATER AND PG/ASTM WATER AT 93 C[(a)]

Solution	Anode/Cathode	Potential, V(SCE) Anode/Cathode	Galvanic Current, $\mu A/cm^2$
EG/ASTM water	6061/1100	-0.322/-0.670	0.3
EG/ASTM water	3003/1100	-0.265/-0.650	0.6
EG/ASTM water	3003/6061	-0.350/-0.550	<0.1
EG/ASTM water	444/1100	-0.040/-0.690	12.9
EG/ASTM water	444/3003	0.035/-0.680	16.5
EG/ASTM water	444/6061	0.055/-0.675	14.5
EG/ASTM water	1018/1100	-0.725/-0.843	1.0
EG/ASTM water	1018/3003	-0.715/-0.885	1.4
EG/ASTM water	1018/6061	-0.715/-0.855	1.2
EG/ASTM water	122/1018	-0.490/-0.695	2.2
EG/ASTM water	444/1018	-0.615/-0.700	19.9
EG/ASTM water	444/122	0.110/ 0.028	6.1
PG/ASTM water	6061/1100	-0.500/-0.660	0.1
PG/ASTM water	1100/3003	-0.570/-0.833	<0.1
PG/ASTM water	6061/3003	-0.500/-0.810	<0.1
PG/ASTM water	444/1100	0.015/-0.690	15.7
PG/ASTM water	444/3003	0.040/-0.700	22.3
PG/ASTM water	444/6061	-0.150/-0.679	6.4
PG/ASTM water	1018/1100	-0.701/-0.718	<0.1
PG/ASTM water	1018/3003	-0.715/-0.800	<0.1
PG/ASTM water	6061/1018	-0.590/-0.718	0.3
PG/ASTM water	122/1018	-0.195/-0.700	2.9
PG/ASTM water	444/1018	-0.672/-0.690	2.9
PG/ASTM water	444/122	0.170/-0.020	5.7

(a) Readings taken after about 500 hours of exposure. Potentials measured after electrically uncoupling the electrodes, which were of equal areas.

DISCUSSION

As stated in the Introduction, the philosophy of this research was to measure corrosion under relatively extreme, or near-worst case, operating conditions anticipated for non-concentrating solar collectors. The data thus reflect corrosion behavior under non-ideal operation, and specifically, in the absence of corrosion inhibitors. These data are applicable to systems in which corrosion inhibitors and/or buffering capacity are depleted, provided such depletion does not accelerate the rate of corrosion above that encountered in uninhibited solutions. The data also reflect the detrimental influence of chloride ion, which is the species that probably will cause the most frequent and severe corrosion problems in actual operating collectors. In this regard, its effects were studied at sufficiently high concentrations to identify tolerable limits for the exposure conditions used in this work. It should be noted that other deleterious species, such as dissolved copper and iron, were not investigated; in another study[4] dissolved copper and iron were shown to cause pitting and accelerated general attack, respectively, of aluminum alloys under simulated solar collector exposure. Also the effects of drain-down were not characterized; drain-down can accelerate corrosion under certain conditions, because it concentrates ionic species and increases availability of atmospheric oxygen. Nevertheless, the sustained temperature of 100 C, presence of turbulent flow, and abundance of dissolved oxygen duplicated harsh operating conditions.

Corrosion Under Dynamic Flow

The data in Tables 5 through 7 are particularly revealing because they indicate relative anticipated corrosion rates in solar collectors under near-worst case conditions. If a tolerable corrosion rate is taken as 89 μm/yr (0.0035 in/yr), which will yield about a 10 year lifetime for tubing with 889 μm (0.035 in) thick walls, then it is apparent that T444 stainless steel would be satisfactory under all conditions that were studied (Table 5).

The high chromium and molybdenum contents of this alloy rendered it virtually inert in all solutions. Conversely, copper 122 corroded at prohibitively high rates in EG solutions, presumably because of the ready availability of dissolved oxygen. Because of the noble corrosion potential of copper, its corrosion rate probably would have been less in deaerated solutions (although this statement is not supported by apparent PR behavior). However, the influence of glycolic degradation products on removal of the protective corrosion film on copper is not established, and this phenomenon could conceivably sustain corrosion in the absence of air.

A protective film possibly would have developed on the inner copper tube surfaces during longer exposures in the presence of dissolved oxygen, and thereby reduced the corrosion rates substantially. It was not practicable to determine this possibility because of the very long exposure times that would have been required. On the other hand, examination of the freely exposed surfaces of copper crevice coupons indicated the presence of a thick, porous, non-protective film after 500 hours exposure. It is suspected that the combined influence of acidification and chloride ion prevented formation of protective Cu_2O. The rather large weight losses of about 8 mg/cm^2 measured during descaling copper tube specimens also suggest the presence of thick and non-protective films.

The large corrosion rates of 1018 steel indicate the need for proper inhibition of solar collector systems containing ferrous, non-stainless components. The smaller corrosion rate in Experiment 2 may have resulted from the increased pH and buffering capacity of the full strength ASTM water, which would have delayed acidification.

The corrosivity of PG/water solutions toward copper and steel was marginally less than that of EG/water solutions for the anion concentrations that were investigated. This factor, and its lesser toxicity, constitute some advantage over EG for use in certain types of solar collector systems.

The pit densities listed in Table 6 show a very high incidence of pit initiation under most exposure conditions. However, the individual pits were very shallow, and it even can be argued that a 3 or 4 μm deep cavity

is not yet a pit. There is undoubtedly a cause and effect relationship between the high density and shallow depths, as first proposed by Mears and Brown[5]. It is conceivable that the flowing action of the solution continually flushed the pits free of the corrosive electrolyte that developed within them, causing high densities but shallow depths.

The pitting propensity of 1100 and 3003 was similar and considerably less than that of the more highly alloyed 6061 in the dilute solutions, although in EG/ASTM water 1100 was noticeably superior to 3003. More quantitative comparisons are possible with the computed pitting constant, k, in Table 7. Larger k values denote a stronger dependence of pit depth on the cube root of exposure time, and thus greater susceptibility to pitting. The values of k for 6061 alloy were consistently higher than those for the other two alloys, and they varied substantially with solution composition. These values clearly show the detrimental effects of chloride ion on pitting corrosions. (The other anions present, namely, sulfate and bicarbonate, do not stimulate pitting of aluminum alloys as strongly as chloride). Specifically, k values increased sharply as the dissolved chloride level reached 50 ppm in EG/ASTM water. A concentration of 50 ppm chloride in the glycol solution corresponds to 100 ppm in the water itself. This is less than the chloride concentration present in many tap waters in the United States. The effect on k of increasing chloride from 0 to 10 ppm, EG/distilled water versus EG/20 percent ASTM water, was much smaller. Comparison of k values in EG and PG solutions provides a clear indication of the greater corrosivity of EG, and shows that the difference is not large. The last column shows that even alloy 6061, the most susceptible to pitting, would allow a design lifetime exceeding 20 years in every solution except EG/ASTM water, and presumably PG/ASTM water. A small change in the exponent of time, t, in Equation 1 would not change the preceding statement because of the very large safety factor present in the calculated penetration times. For example, for 6061 alloy to fail in 20 years in EG/distilled water by penetration through a wall thickness of 508 μm, the exponent in Equation 1 would have to be increased from 0.33 to about 0.50.

It is significant that Task 3[2] research results showed much deeper pits on aluminum alloys than those reported in Table 6. For example, after 1750 hours in aerated EG/distilled water at 100 C the maximum pit depths in 1100, 3003, and 6061 alloys were 530, 450, and 240 μm, respectively. At least two possible explanations exist for the more severe pitting in this companion study. First, the exposure of 1750 hours resulted in lower final pH values, generally in the range 3.3 to 3.8, and these lower pH's may be responsible for the greater attack. Second, the stagnant exposure conditions may have promoted the growth of fewer pits and to deeper depths than the dynamic flow used in the present investigation.

It is conceivable that aluminum alloys could be used successfully in uninhibited flowing EG and PG solutions, provided the only corrosive species is chloride ion and its concentration is kept well below 50 ppm. However, the possibilities of enhanced pitting during periods of stagnant flow, from possible contamination by additional chloride, and from accumulation of Cu^{++} or Fe^{+++} ions[4] strongly dictate the need for adequate chemical inhibition of corrosion in commercial aluminum collector systems.

The data in Tables 3 and 4 raise a question concerning the usefulness of PR as a quantitative indicator of corrosion. For example, PR was relatively low on T444 stainless steel, yet no measurable corrosion occurred on this alloy. Apparently, a redox reaction occurred on the steel that gave rise to the large measured currents. The nature of this reaction is not known; it may have resulted from accumulation of acidic degradation products of the glycols, or possibly a Cu^{+}/Cu^{++} couple was operating as a result of corrosion of the copper tube specimens. PR has been used successfully in inhibited glycol solutions to measure corrosion rates of aluminum and other alloys[6]; therefore, its utility in collector systems cannot lightly be dismissed. Additional research is needed to define those conditions under which PR provides a reliable measure of corrosion behavior. Lack of accurate Tafel data in the present study prevented resolution of this question.

The acidification of the glycol solutions to pH values below 5 after only 300 to 400 hours of exposure at 100 C is the result of relatively rapid degradation of these solutions. Acidification may also have been

assisted by hydrolysis of corrosion products; however, results of Task 3 research showed that acidification also occurs in the absence of metals, although at slower rates. Task 3 also demonstrated that acidification continued for many hundreds of hours and, therefore, the pH values of 4+ listed in Tables 3 and 4 should not be considered the minimum attainable by these solutions. The relatively rapid rates of acidification of EG solutions, the initially low pH of the PG solutions, and the known deleterious effects of acidic solutions on the corrosion of aluminum and copper alloys underscore the advisability of buffering glycol solutions adequately to a near-neutral or mildly alkaline pH.

Corrosion potential qualitatively reflected the pitting behavior of the aluminum alloys. Specifically, those instances in which k exceeded 10 $\mu m/hr^{1/3}$ also resulted in active values of E_{corr}, usually between -0.90 and -1.00 V(SCE). Values of k of 3 $\mu m/hr^{1/3}$ or less correlate with E_{corr}'s more positive than about -0.20 V(SCE). Thus, E_{corr} may be useful as an indicator of loss of passivity and rapid pitting in aluminum collectors; a measurement device based on this principle is being evaluated elsewhere for possible use in aluminum collectors[7].

The lack of effect of heat transfer on corrosion rate is significant, because the maximum flux of 4730 Wm^2 is about that anticipated in tube-and-fin solar collectors. However, certain types of corrosion inhibitors are influenced by heat transfer; thus, heat transfer should be included in any laboratory study of corrosion inhibitors, unless there is evidence showing that it exerts no significant influence.

Crevice Corrosion

Results in Table 10 show that crevice corrosion could be a severe problem with aluminum alloys in uninhibited glycol solutions, especially those containing 50 ppm or more of chloride ion. Crevices in commercial collectors can arise as a result of fabrication technique, such as at welded seams, and through assembly, such as at attachment points for hoses and tubing. Because of the known tendency of aluminum for crevice corrosion,

the use of corrosion inhibitors is advisable. A preferable deterrent, however, is avoidance of crevices in the collector system.

It should not be assumed that the absence of crevice attack in Table 10 implies absolute immunity. It is conceivable that a different surface treatment, or greater number of replicate specimens, would have resulted in some attack. Nevertheless, the data in Table 10 show relative susceptibilities. Note that in the case of 6061 alloy, PTFE-metal crevices corroded more severely than metal-metal crevices.

Galvanic Coupling

The accelerating influence on corrosion of galvanic coupling can be calculated, as follows. A shift in E_{corr} of the anodic member of a galvanic couple by more than about 25 mV results in the measured galvanic current being nearly equal to the corrosion rate of the anode. Such large shifts were measured for couples between aluminum alloys and other metals, 3003 and 6061 aluminum alloys, and in certain other couples. Faraday's law can be used to show that for aluminum, a corrosion current of 1 $\mu A/cm^2$ corresponds to a metal recession rate of 10.9 μm/yr, based on the overall reaction:

$$Al = Al^{+++} + 3e \qquad (2)$$

and not considering the influence of alloying elements in the 3003 and 6061 alloys. Also ignored are other possible oxidation reactions that may occur in degraded glycol solutions, as referred to earlier. If a 51 μm/yr (0.002 in/yr) corrosion rate is taken on the allowable limit, then a galvanic current of 4.6 $\mu m/cm^2$ is the maximum permissible. However, the common form of corrosion of aluminum alloys is pitting, and the current densities within pits are much higher than the nominal value calculated over the entire specimen area. Therefore, galvanic corrosion of almost any magnitude should be avoided with aluminum alloys.

Galvanic couples between aluminum alloys and copper were not investigated during this research. Such couples are to be avoided at all

costs, since prior experience in many applications has shown that severe pitting of the aluminum member occurs, primarily as a result of the high concentration of cupric ion and noble E_{corr} of copper.

For copper, the calculated maximum permissible corrosion current is 4.4 $\mu A/cm^2$; therefore, coupling to T444 stainless steel would not be advisable.

The influence of type of glycol on the nature of galvanic corrosion was, in some cases, quite pronounced. For example, changing from EG to PG caused a reversal in polarity of couples involving 1100/3003, 3003/6061, and 1018/6061, and it caused lower galvanic currents to flow in others. Although uninhibited PG solutions appear to offer some advantage over EG solutions with respect to crevice corrosion, the presence of corrosion inhibitors probably would reduce the difference between their relative corrosivities.

CONCLUSIONS

This research has provided information about corrosion in solar collector systems under simulated harsh operating conditions. The following points are especially significant:

(1) Type 444 stainless steel corroded at negligibly small rates (less than 1 μm/yr) under all exposure conditions that were evaluated. It is a promising alloy for use in uninhibited collector systems, or in those that operate under harsh conditions or with poor anticipated maintenance.

(2) Aluminum alloys 1100, 3003, and 6061 pitted in EG and PG solutions, but at acceptable rates provided the chloride concentration is kept well below 50 ppm. However, because of possible contamination of solutions in commercial solar collector systems, and because pitting of aluminum

alloys is more rapid under stagnant exposure, the use of adequate corrosion inhibition is strongly recommended for satisfactory performance.

(3) Copper corroded at prohibitively high rates in EG solutions and at near-prohibitive rates in PG solutions. Exclusion of dissolved oxygen might have reduced the corrosion rates. The impossibility of insuring oxygen-free solutions in commercial collector systems, and the accelerating effects of glycol acidification on corrosion rates, mandate the use of corrosion inhibitors.

(4) Crevice corrosion can be a severe problem with aluminum alloys in glycol solutions. It does not appear to threaten the integrity of copper and T444 stainless steel.

(5) Galvanic coupling in glycol solutions can seriously accelerate the corrosion rates of aluminum alloys, especially if the other member of the couple is much more noble. Couples between copper and stainless steel also should be avoided.

(6) Aqueous glycol solutions, both EG and PG, underwent acidification during several hundred hours of exposure to air at 100 C. The resulting pH values, in the range of 4 to 5, can accelerate corrosion rates. Therefore, glycol solutions should be buffered and inhibited when used in aluminum or copper collectors.

(7) PG appeared to produce somewhat smaller rates of pitting and general corrosion on aluminum alloys and copper. These differences may

become insignificant if the glycols are properly inhibited and buffered to minimize corrosion.

(8) Polarization resistance measurements did not accurately indicate the corrosion behavior of T444 in glycol solutions. Its suitability for corrosion monitoring of aluminum alloys and copper needs additional investigation.

(9) Heat transfer rates as large as 4730 W/m^2 did not substantially influence corrosion of aluminum alloys or copper in uninhibited glycol solutions.

In principle, and under unrealistically ideal conditions, it would be possible to achieve a 10 to 20 year lifetime of aluminum and copper collectors with uninhibited EG and PG solutions, provided contamination by chloride, metal ions, and oxygen is prevented, and crevice corrosion and galvanic coupling are minimized. However, the near-impossibility of maintaining these conditions throughout the life of the collector system underscores the advisability of using adequate corrosion inhibitors and buffering capacity. The need for such inhibition is much less critical in a T444 stainless steel system.

ACKNOWLEDGMENTS

The author is pleased to acknowledge the technical assistance rendered by G. A. Breeze. Several technical discussions were held with P. W. Brown of the National Bureau of Standards, and one with R. Lindberg of Reynolds Metals Company. J. D. Redmond, of Climax Molybdenum Company, and W. I. Weed, of Jones and Laughlin Steel, graciously supplied the specimens of T444 stainless steel.

REFERENCES

1. Clifford, J. E., and Diegle, R. B., Technical Progress Report, Task 1 of Solar Collector Studies for Solar Heating and Cooling Applications, United States Department of Energy, Contract No. DE-AC04-79CS10510, September, 1979.
2. Beavers, J. A., and Diegle, R. B., Technical Progress Report, Task 3 of Solar Collector Studies for Solar Heating and Cooling Applications, United States Department of Energy, Contract No. DE-AC04-79CS10510, September, 1979.
3. Goddard, H. P., Jepson, W. B., Bothwell, M. R., and Kane, R. L., The Corrosion of Light Metals, John Wiley and Sons, Inc., New York (1967), p.60.
4. Wong, D., Swette, L., and Cocks, F. H., J. Electrochem. Soc., 126 (1), 11 (1979).
5. Mears, R. B., and Brown, R. H., Ind. Eng. Chem., 29 (70), 1087 (1937).
6. Walker, M. S., and France, W. K., Jr., Materials Protection, 8 (9), 47 (1969).
7. Cheng, C., personal communication.

APPENDIX

VARIATIONS OF POTENTIAL AND CURRENT WITH TIME DURING GALVANIC COUPLING EXPERIMENTS

Figures A-1 through A-8 show variations of uncoupled corrosion potential and galvanic current with exposure time in aerated EG/ASTM water and PG/ASTM water solutions for galvanic couples between various alloys.

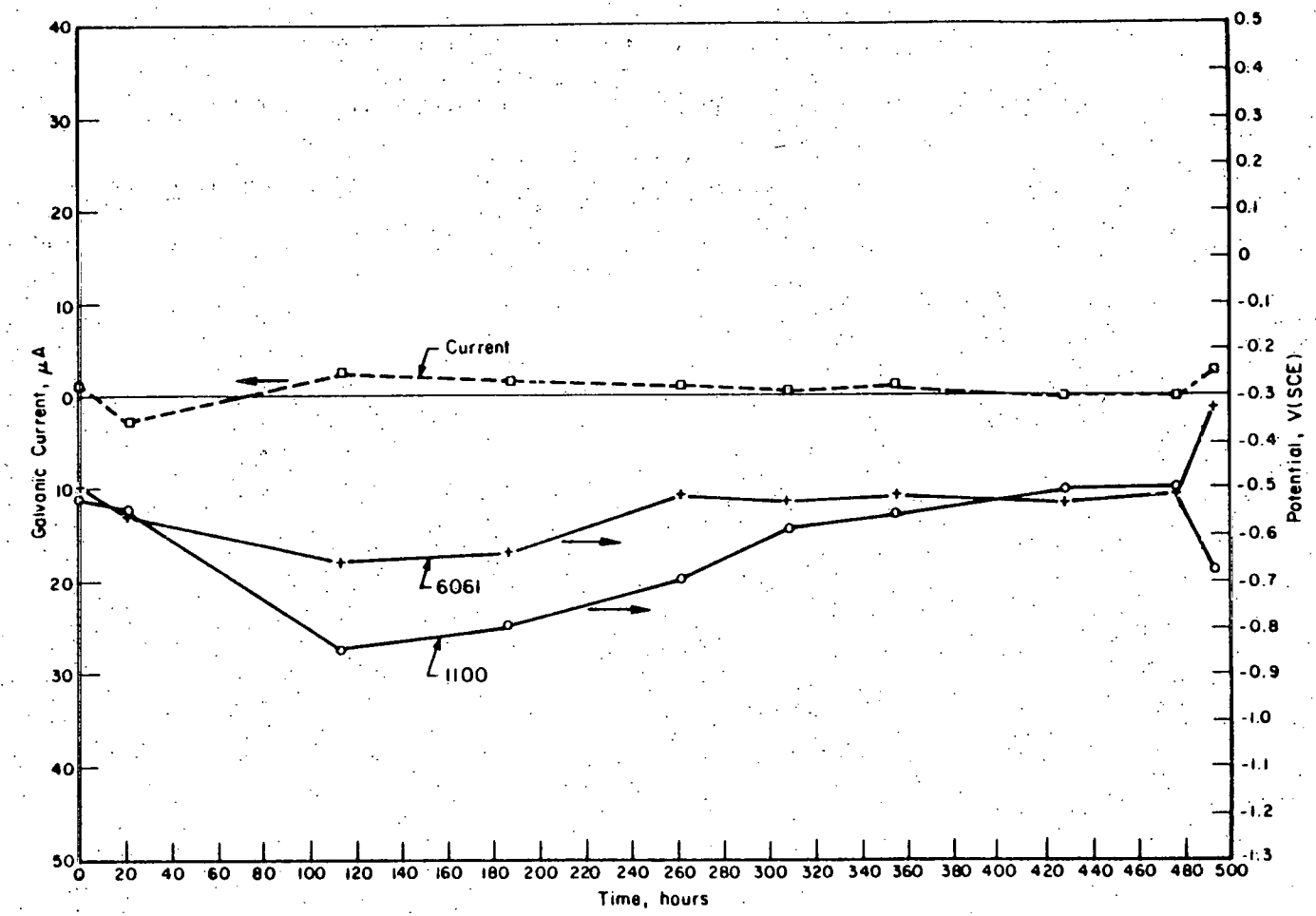

FIGURE A-1. VARIATION OF POTENTIALS AND CURRENT WITH INCREASING EXPOSURE TIME IN AERATED EG/ASTM WATER AT 93 C FOR GALVANIC COUPLE OF Al 1100 AND 6061 ALLOYS

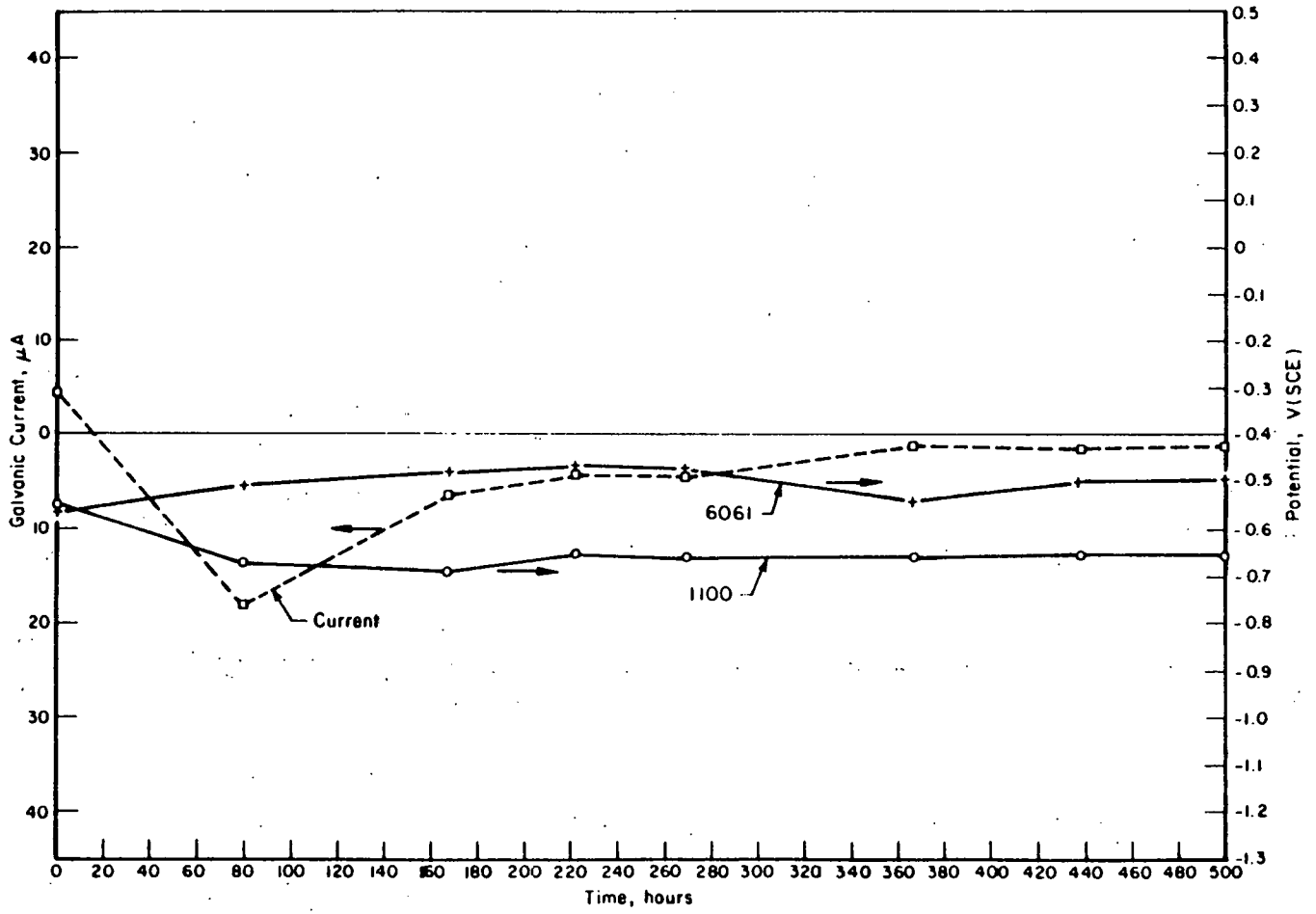

FIGURE A-2. VARIATION OF POTENTIALS AND CURRENT WITH INCREASING EXPOSURE TIME IN AERATED PG/ASTM WATER AT 93 C FOR GALVANIC COUPLE OF A1 1100 AND 6061 ALLOYS

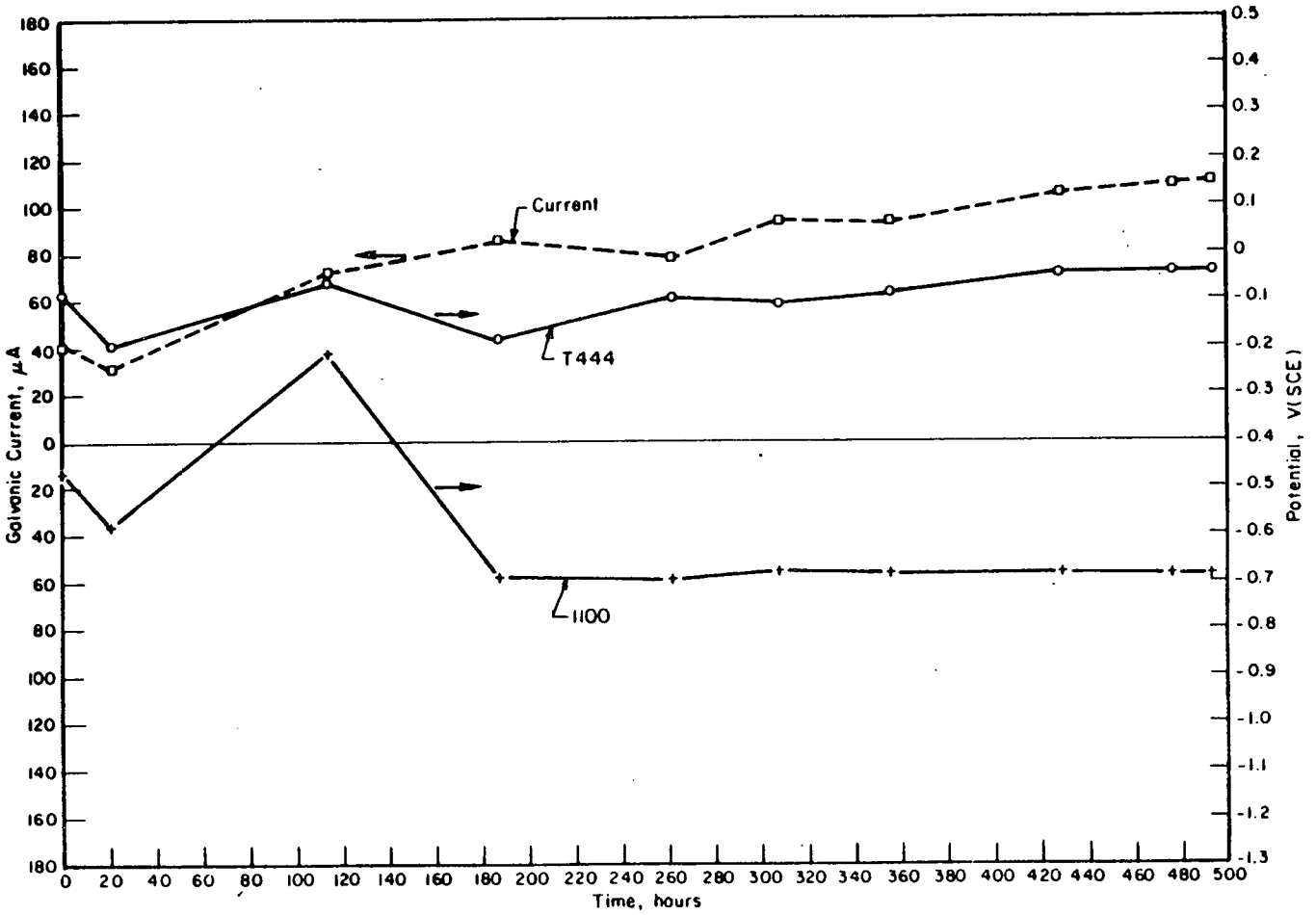

FIGURE A-3. VARIATION OF POTENTIALS AND CURRENT WITH INCREASING EXPOSURE TIME IN AERATED EG/ASTM WATER AT 93 C FOR GALVANIC COUPLE OF A1 1100 AND T444 STAINLESS STEEL

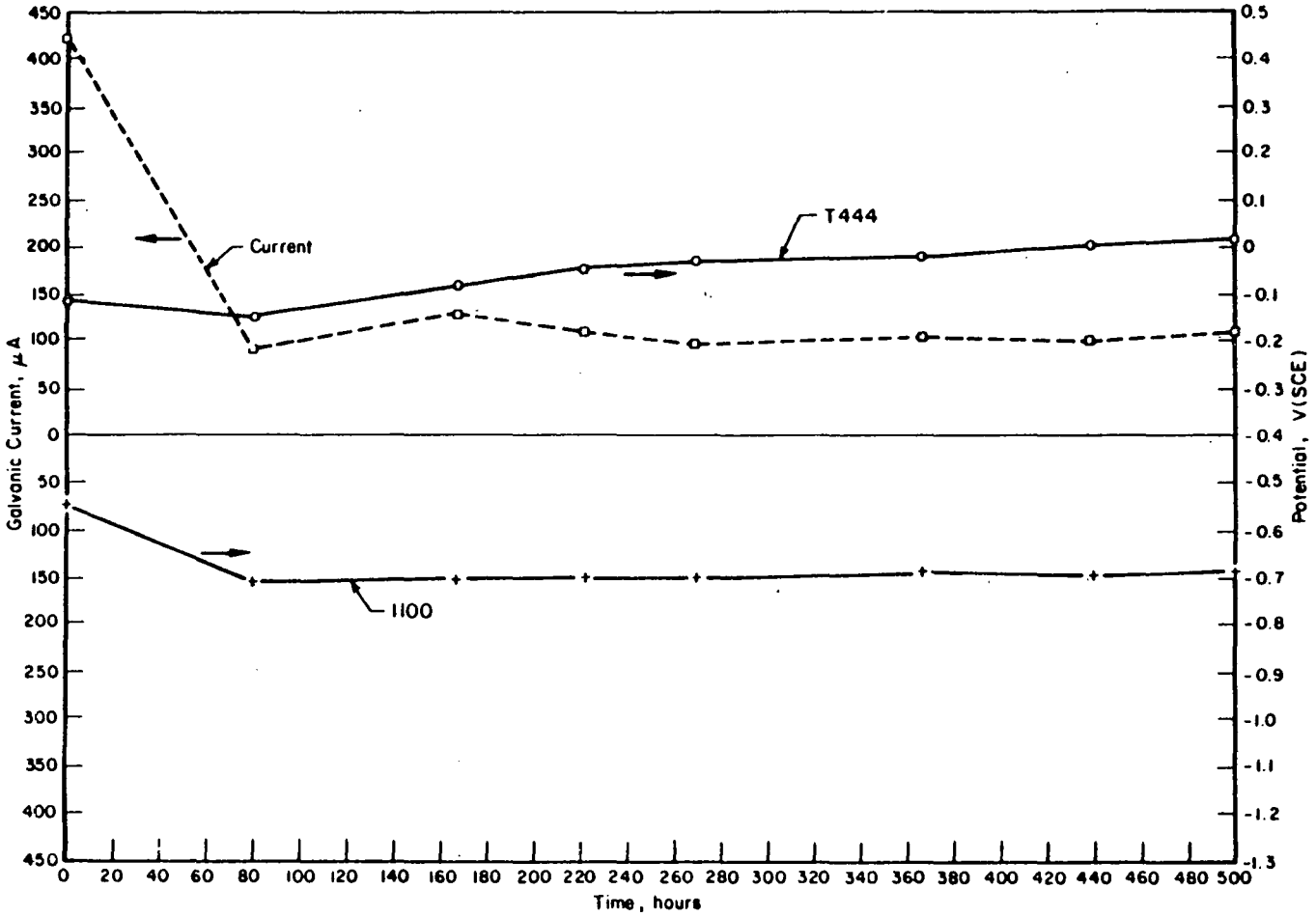

FIGURE A-4: VARIATION OF POTENTIALS AND CURRENT WITH INCREASING EXPOSURE TIME IN AERATED PG/ASTM WATER AT 93 C FOR GALVANIC COUPLE OF Al 1100 AND T444 STAINLESS STEEL

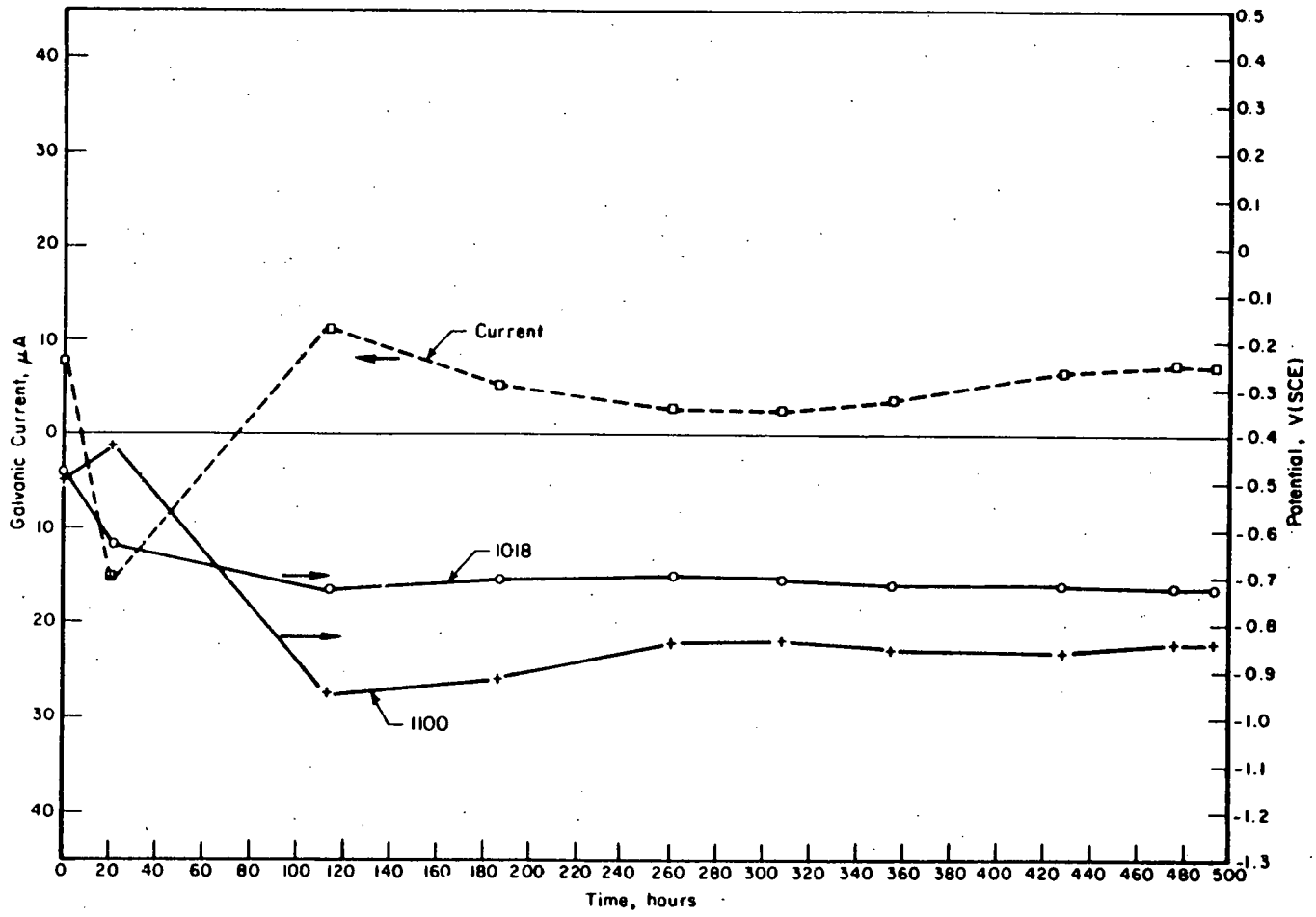

FIGURE A-5. VARIATION OF POTENTIALS AND CURRENT WITH INCREASING EXPOSURE TIME IN AERATED EG/ASTM WATER AT 93 C FOR GALVANIC COUPLE OF A1 1100 AND 1018 STEEL

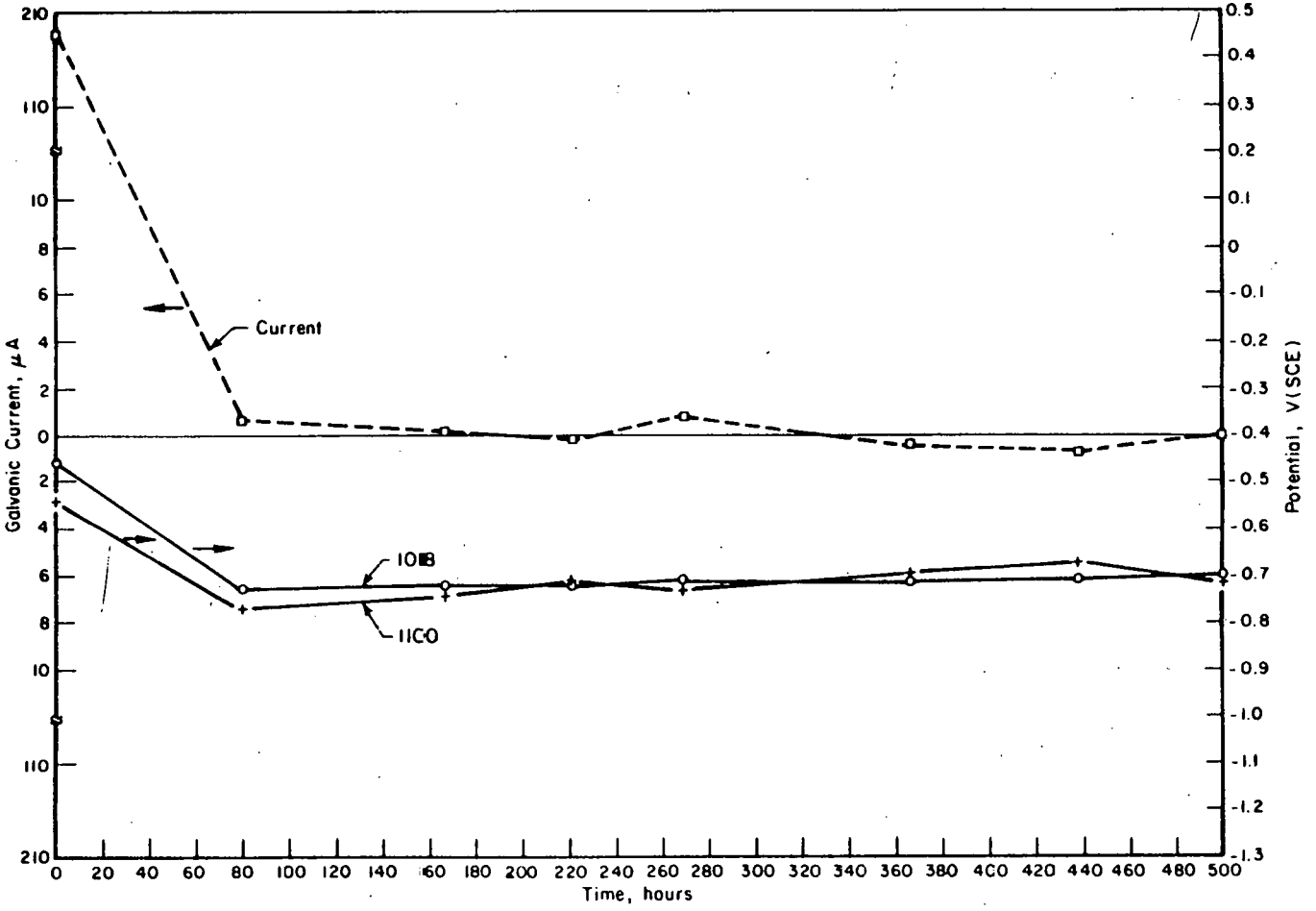

FIGURE A-6. VARIATION OF POTENTIALS AND CURRENT WITH INCREASING EXPOSURE TIME IN AERATED PG/ASTM WATER AT 93 C FOR GALVANIC COUPLE OF A1 1100 AND 1018 STEEL

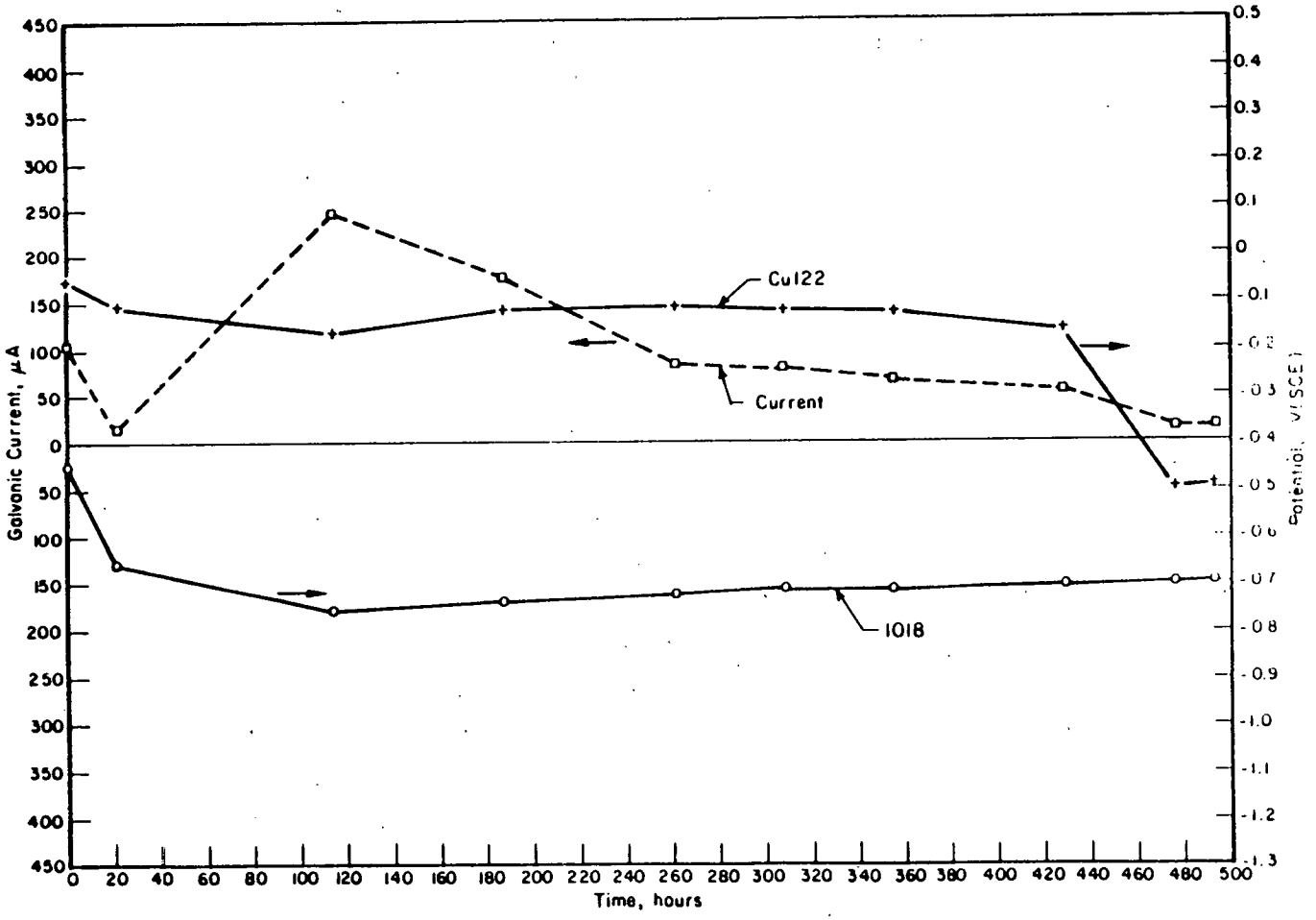

FIGURE A-7. VARIATION OF POTENTIALS AND CURRENT WITH INCREASING EXPOSURE TIME IN AERATED EG/ASTM WATER AT 93 C FOR GALVANIC COUPLE OF Cu 122 AND 1018 STEEL

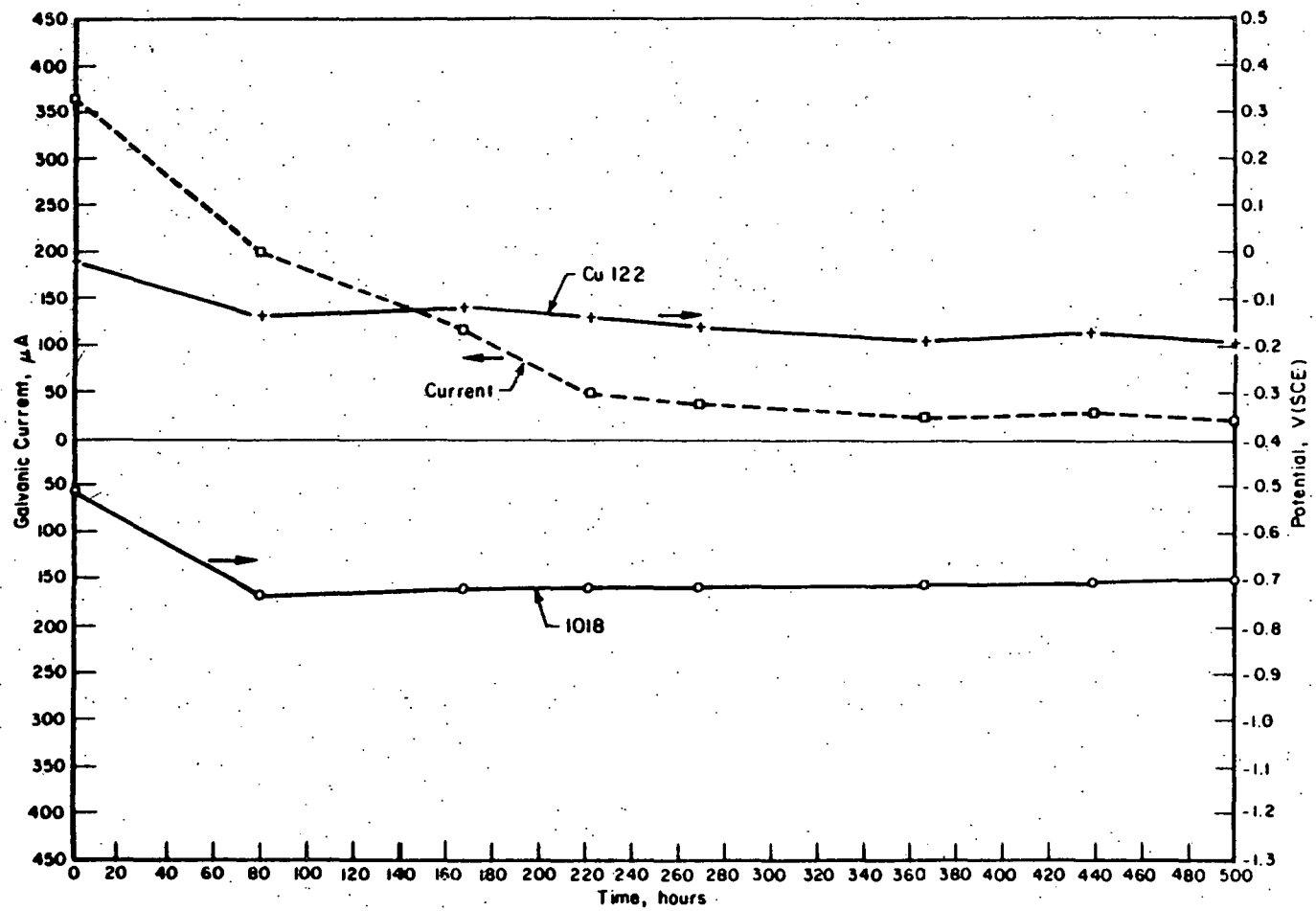

FIGURE A-8. VAEIATION OF POTENTIALS AND CURRENT WITH INCREASING EXPOSURE TIME IN AERATED PG/ASTM WATER AT 93 C FOR GALVANIC COUPLE OF Cu 122 AND 1018 STEEL